

# The NEU Meta-Algorithm for Geometric Learning with Applications in Finance

ANASTASIS KRATSIOS\* CODY B. HYNDMAN\*

August 31, 2018

## Abstract

We introduce a meta-algorithm, called non-Euclidean upgrading (NEU), which learns algorithm-specific geometries to improve the training and validation set performance of a wide class of learning algorithms. Our approach is based on iteratively performing local reconfigurations of the space in which the data lie. These reconfigurations build universal approximation and universal reconfiguration properties into the new algorithm being learned. This allows any set of features to be learned by the new algorithm to arbitrary precision. The training and validation set performance of NEU is investigated through implementations predicting the relationship between select stock prices as well as finding low-dimensional representations of the German Bond yield curve.

*Keywords:* Machine Learning, Non-Euclidean Geometry, Statistical Learning, Learning Algorithms, Optimizations, Regression, Dimensionality Reduction, Meta-Algorithms, Algebraic-Topology, Principal Geodesic Analysis.

**Mathematics Subject Classification (2010):** 60D05, 91G60, 62G08, 65D15, 62H25, 91G80.

## 1 Introduction

Many statistical and learning algorithms such as ordinary linear regression and PCA admit linear algebraic formulations making them quick to execute. Their inability to capture non-linear features has motivated several non-linear generalizations. Non-linear generalizations of linear models require alternative, computationally costly, estimation procedures. Generalized additive models (GAM) and artificial neural networks (ANN) are examples of non-linear generalizations of linear regression that come with a significant increase in computational cost (see [14, Chapters 9 and 11] for a discussion of these methods).

---

\*Department of Mathematics and Statistics, Concordia University, 1455 Boulevard de Maisonneuve Ouest, Montréal, Québec, Canada H3G 1M8. emails: anastasis.kratsios@mail.concordia.ca, cody.hyndman@concordia.ca

This research was supported by the Natural Sciences and Engineering Research Council of Canada (NSERC). The authors thank Alina Stancu (Concordia University) for helpful discussions.

Patterns in the data are typically interpreted as a function relating explanatory inputs to the observations which they explain. Alternatively, a pattern can be interpreted as the positioning of points in space. Since a function’s graph is a specific set of points in space, interpreting a pattern as a configuration of points in space is more general than interpreting it as a function. The non-Euclidean Upgrading (NEU) methodology introduced in this paper can learn any configuration of data. As a consequence, two versions of the universal approximation property (see [5] for details) of ANNs is also recovered.

Non-Euclidean Upgrading (NEU) is a meta-algorithm. Meta-algorithms are algorithms whose inputs and outputs are other algorithms. For example, the Boosting meta-algorithm of [26] efficiently combines learning algorithms to build a more accurate new learning algorithm. Bagging, as introduced in [3], is another meta-algorithm which generates bootstrapped samples from a given dataset, performs the input algorithm on those bootstrapped samples, and aggregates each of the predictions into a lower-variance estimate. NEU is also a meta-algorithm which inputs a learning algorithm and a dataset, and outputs a new algorithm with the universal approximation property built into it. Applying NEU to simple linear algorithms produces algorithms which are interpretable, have a low computational burden, and can predict any pattern to arbitrary precision once trained.

NEU works by first segmenting the input data into training and validation components, then performing local perturbations on the space on which the data is defined, executing the learning algorithm on the perturbed training and validation data sets, and evaluating if the validation set performance has increased. The procedure continues iteratively, stopping once the validation set performance begins to drop.

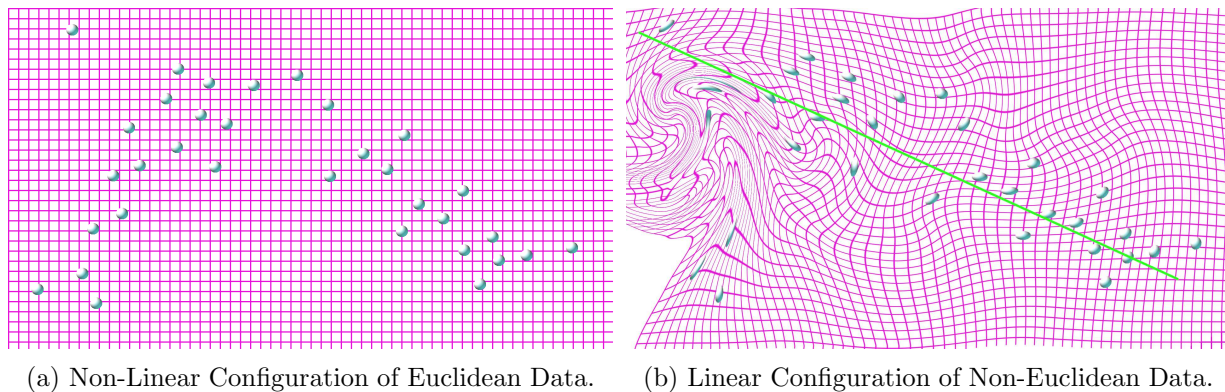


Figure 1: Visualization of Reconfiguration of the Data.

Figure 1 illustrates how perturbing  $\mathbb{R}^2$  reconfigures the given dataset and allows for a linear regression to explain a non-linear relationship. After linear regression is performed, the transformations to  $\mathbb{R}^2$  are inverted and the linear predictor becomes non-linear. This illustration is analogous to the non-Euclidean regression proposed in [10] with the central difference being that our methodology learns the geometry of the problem whereas the algorithm in [10] relies on a prespecified geometry.

Applying NEU to principal component analysis (PCA) generates an analogue of the principal geodesic analysis of [11] where the geometry is learned from the data. Applying NEU to the

unscented Kalman filtering algorithm of [16] or to the geometric GARCH framework of [13] produces analogues of those algorithms but without a prespecified geometry. There are many other potential applications of NEU in statistics and machine learning.

We consider two examples from finance. The first example considers the use of principal component analysis (PCA) on German bond data. Using NEU on PCA shows that one NEU-principal component performs better than 4 standard principal components.

The second example from finance considers the relationship between Apple stock price and the stock prices of companies related to Apple. Using NEU on linear regression provides better out-of-sample predictions than the LASSO, Ridge regression, and non-linear extensions of Elastic-Net (ENET) procedures. While we consider only two examples from finance to illustrate NEU, the generality and flexibility should allow for similar performance gains in other areas of financial statistics and machine learning.

The remainder of this paper is organized as follows. Section 2 introduces the mathematical framework for non-Euclidean upgrading, the main results regarding the technique’s flexibility, and predictive performance enhancement are proven. Section 3 investigates the empirical performance of non-Euclidean upgrading on the two examples from finance. The relationship between Apple stock price and the stock price of related companies can be better explained training sets and validation sets using non-Euclidean upgraded regression. Parallels are drawn to the non-Euclidean generalizations of regression and principal geodesic analysis developed in [10] and [11], respectively. We adjoin an appendix with two sections, the first lists the regularity assumptions made and the second contains certain technical proofs.

## 2 Non-Euclidean Upgrading

This section introduces and develops the NEU meta-algorithm. Reconfigurations are first introduced and a universal approximation property is proven. The NEU meta-algorithm is then introduced and its performance gain property is proven.

### 2.1 Reconfiguration

For the remainder of this paper, a dataset will be comprised of training and validation sets. The training set will be denoted by  $X^I = \{X_1^I, \dots, X_{N_I}^I\}$  and the validation set will be denoted by  $X^O = \{X_1^O, \dots, X_{N_O}^O\}$ , where  $N_I$  and  $N_O$  are non-negative integers and  $N_I \geq 1$ .

Reconfigurations perturbing the dataset are smooth maps from  $\mathbb{R}^D$  back into itself, smooth autodiffeomorphisms, which satisfy certain local properties. These are defined as follows.

**Definition 2.1** (Reconfiguration Map) *Let  $\Theta$  be an open subset of  $\mathbb{R}^m$  and  $\mathcal{S}$  be a star-shaped domain in  $\mathbb{R}^D$  of dimension  $D$ . A reconfiguration on  $\mathcal{S}$  is a map*

$$\begin{aligned} \xi : \mathcal{S} \times \Theta &\rightarrow \mathcal{S}, \\ (x, \theta) &\mapsto \xi(x|\theta) \end{aligned}$$

*satisfying the following properties:*

- (i) **Invertibility:** For every  $\theta \in \Theta$ , the map  $f_\theta(x) \triangleq \xi(x|\theta)$  is a bijection,
- (ii) **Smoothness:** For every  $\theta \in \Theta$ , the maps  $f_\theta(x)$ , and  $f_\theta^{-1}$  are continuously differentiable,
- (iii) **Smooth Parametrization:** For every  $x$  in  $\mathbb{R}^D$ , the map  $\theta \mapsto \xi(x|\theta)$  is continuously differentiable,
- (iv) **Local Transience:** For every  $x, y, z$  in  $\mathcal{S}$  with  $d(x, y) < d(x, z)$ , there exists  $\theta \in \Theta$  such that

$$\xi(x|\theta) = y$$

$$\xi(z|\theta) = z,$$

where  $d(\cdot, \cdot)$  is the Euclidean distance on  $\mathbb{R}^D$ .

- (v) **Identity:** The subset  $\Theta_0 \triangleq \{\theta \in \Theta : \xi(x|\theta) = x, \forall x \in \mathbb{R}^D\}$  of  $\Theta$  is non-empty.

The central example of a reconfiguration map, is a rapidly decaying rotation concentrated on a disc. These rotations slow exponentially as the boundary of the disc is approached. Beyond the disc's boundary the reconfiguration map becomes the identity transformation. Rapidly decaying rotations are illustrated by Figure 2.

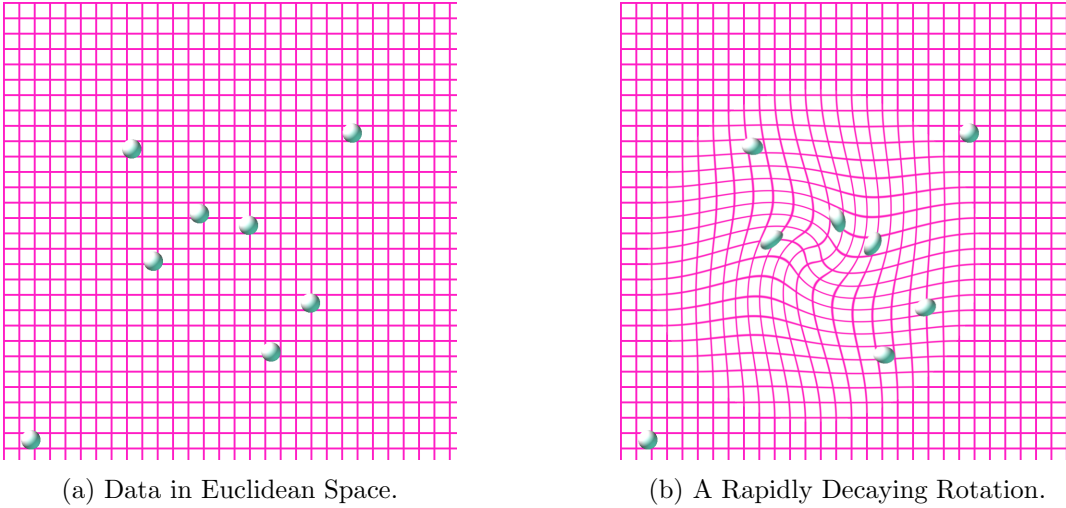


Figure 2: Visualization of Rapidly Decaying Rotations.

**Definition 2.2** (Rapidly Decaying-Rotations) Let  $\mathfrak{so}(D)$  denote the set of  $D \times D$  skew-symmetric matrices and set  $\Theta \triangleq \mathbb{R}^D \times (0, \infty) \times \mathfrak{so}(D)$ . A rapidly decaying rotation is the map  $\xi$  defined by

$$\begin{aligned} \xi : \mathbb{R}^D \times \Theta &\rightarrow \mathbb{R}^D \\ \xi(x|(c, \sigma, X)) &\mapsto \exp(\psi(\|x - c\|; \sigma)X)(x - c) + c, \end{aligned} \quad (2.1)$$

where  $\psi$  is the Gaussian bump-function supported on the unit sphere of radius  $\sigma$  centered at the point  $c \in \mathbb{R}^D$ , defined by

$$\psi(x; \sigma) \triangleq \begin{cases} \exp\left(\frac{-\sigma}{\sigma - \|x\|^2}\right) & : \|x\| < \sigma \\ 0 & : \text{else,} \end{cases} \quad (2.2)$$

and  $\exp$  is the matrix exponential map.

**Proposition 2.3.** Rapidly decaying rotations are reconfiguration maps on  $\mathbb{R}^D$ . Moreover, the inverse of  $\xi(\cdot|c, \sigma, X)$  is

$$\Phi(x|c, \sigma, X) = \exp(-X\psi(\|y\|; \sigma))(x - c) + c,$$

where  $y$  is the image of  $x$  under  $\Phi(\cdot|c, \sigma, X)$ .

*Proof.* The proof is deferred to the appendix □

**Remark 2.4** (Geometric Interpretation). The rapidly decaying rotations are interpolations between a rotation and the identity map interior to the disc of radius  $\sigma$ , centered at  $c$ . However, the interpolation does not take place in  $\mathbb{R}^D$ , but instead happens within the lie algebra  $\mathfrak{so}(D)$  lying tangential to the space of all generalized rotation matrices  $SO(D)$ . This ensures that the map is invertible for all possible parameter choices.

**Definition 2.5** (Planar Micro-Bumps) *A planar micro-bump on  $\mathbb{R}^2$ , is the map  $\xi$  defined by*

$$\begin{aligned} \xi : \mathbb{R}^2 \times \Theta &\rightarrow \mathbb{R}^2 \\ \xi((x_1, x_2)|c, \sigma, X) &\mapsto x + \psi(\|x - c\|; \sigma)X, \end{aligned} \tag{2.3}$$

where  $\Theta = \mathbb{R}^2 \times [0, \infty) \times \mathbb{R}$ .

**Proposition 2.6.** Planar micro-bumps are reconfigurations maps on  $\mathbb{R}^2$ .

*Proof.* The proof is deferred to the appendix □

Data points are deemed poorly placed if moving them increases the validation set performance of a learning algorithm. Iteratively applying reconfiguration maps allows poorly placed data-points to be moved to locations which increase an algorithm’s validation set performance. The local transience property of reconfiguration maps, Definition 2.1 (iv), makes it possible to only move poorly placed data-points while leaving the others fixed. The procedure is summarized as follows.

**Definition 2.7** (Reconfiguration) *Let  $\mathcal{S}$  be a star-shaped domain in  $\mathbb{R}^D$  of dimension  $D$ ,  $\mathcal{M}$  be a smooth sub-manifold of  $\mathbb{R}^D$ , which is diffeomorphic<sup>1</sup> to  $V$ ,  $\Phi$  be a diffeomorphism<sup>2</sup> from  $\mathcal{M}$  onto  $\mathcal{S}$ , let  $\xi$  be a reconfiguration map on  $\mathcal{S}$ , and let  $\theta_0, \dots, \theta_N$  be in  $\Theta$  with  $\theta_0 \in \Theta_0$ . Here  $\Theta_0$  is as in definition 2.1(v). A reconfiguration  $\mathbb{X}$ , is a map from  $\mathcal{M}$  to  $\mathcal{M}$  defined by*

$$\mathbb{X}(x|\theta_1, \dots, \theta_N; \Phi) \triangleq \Phi \left( X^{(N)}(x) \right)$$

where

$$\begin{aligned} X^{(i)}(x) &\triangleq \xi \left( X^{(i-1)}(x)|\theta_i \right); \quad i = 1, \dots, k \\ X^{(0)}(x) &\triangleq \xi(x|\theta_0). \end{aligned}$$

---

<sup>1</sup> The Whitney embedding theorem implies that any smooth manifold is a smooth subset of a Euclidean space. In this paper, a map will be quantified as being smooth if it is once continuously differentiable.

<sup>2</sup> A diffeomorphism is a bijection which is smooth and has a smooth inverse.

Reconfiguring a dataset on  $\mathbb{R}^D$  maps it into new coordinates for the input  $D$ -variables. These coordinates may not be directly interpretable, therefore after performing the learning algorithm and obtaining an estimate in the new coordinate system the reconfiguration must be inverted. This inverse procedure is called deconfiguration.

**Definition 2.8** (Deconfiguration) *Let  $\mathbb{X}$  be a reconfiguration of  $\mathcal{M}$ . The deconfiguration of  $\mathbb{X}$  is the map denoted by  $\mathbb{X}^{-1}$  defined as*

$$\begin{aligned}\mathbb{X}^{-1}(x|\theta_1, \dots, \theta_N; \Phi) &\triangleq \Phi^{-1}\left(X^{(N)}(x)\right) \\ X^{(i)}(x) &\triangleq \xi^{-1}\left(X^{(i-1)}(x)|\theta_{N-1}\right); \quad i = 1, \dots, N \\ X^{(0)}(x) &\triangleq \xi^{-1}(x|\theta_0).\end{aligned}$$

The universal approximation property of neural networks states that certain neural networks can approximate any function to arbitrary precision (see [5]). The first analogous property for reconfiguration states that any dataset can be transformed into any other dataset of equal size.

**Theorem 2.9** (Universal Reconfiguration Property). Assume that  $D > 1$ ,  $\mathcal{S}$  is an open star-shaped domain in  $\mathbb{R}^D$  of dimension  $D$ ,  $\xi$  be a reconfiguration map on  $\mathcal{S}$ , and  $\Phi$  be a diffeomorphism from  $\mathcal{M}$  onto  $\mathcal{S}$ . Let  $X \triangleq \{X_i\}_{i=1}^N$  and  $\tilde{X} \triangleq \{\tilde{X}_i\}_{i=1}^N$  be subsets of  $\mathcal{M}$ . There exists a positive integer  $K$ , and  $\theta_1, \dots, \theta_K$  in  $\Theta$  for which

$$\mathbb{X}(X_i|\theta_1, \dots, \theta_K; \Phi) = \tilde{X}_i,$$

for every  $i$  in  $\{1, \dots, N\}$ .

*Proof.* The proof is deferred to the appendix. □

The universal reconfiguration property implies the following analogues to the universal approximation property of neural networks of [19]. The first captures general functions on a more restricted domain and the second captures a smaller class of functions on a larger domain.

**Corollary 2.10** (Universal Approximation Property). Let  $D_1, D_2$  be positive integers,  $\mathcal{S}$  be a subset of  $\mathbb{R}^{D_1}$  and  $f, g$  be Borel-functions from  $\mathcal{S}$  to  $\mathbb{R}^{D_2}$ . If  $\mathcal{S}$  is diffeomorphic to  $\mathbb{R}^{D_1}$ , then for every countable subset  $Q$  of  $\mathcal{M}$ , probability measure  $\mathbb{P}$  supported on  $Q$ , and every  $n \in \mathbb{N}$ , there exists  $\theta_1^n, \dots, \theta_{N_n}^n \in \Theta$  such that for every  $\epsilon > 0$  there exists a Borel-subset  $\mathcal{S}_\epsilon$  of  $Q$  satisfying

1.  $\sup_{x \in \mathcal{S}_\epsilon} \|f(x) - p \circ \mathbb{X}((x, g(x))|\theta_1^n, \dots, \theta_{N_n}^n)\| < \frac{1}{n}$ ,
2.  $\mathbb{P}(Q - \mathcal{S}_\epsilon) < \epsilon$ .

Here  $p$  is the second canonical projection<sup>3</sup> of  $\mathbb{R}^{D_1+D_2}$  onto  $\mathbb{R}^{D_2}$ . In the limiting case where  $\epsilon = 0$ , the convergence of  $p \circ \mathbb{X}((x, g(x))|\theta_1^n, \dots, \theta_{N_n}^n)$  to  $f(x)$  on  $Q$  is point-wise.

*Proof.* The proof will be deferred to the appendix. □

<sup>3</sup>The second canonical projection of the product space  $X \times Y$  takes a pair  $(x, y)$  to  $y$ , see [20] for details.

**Corollary 2.11** (Universal Smooth Approximation Property). Let  $D_1, D_2$  be positive integers,  $K$  is a regular, convex, compact subset of  $\mathbb{R}^{D_1}$  of dimension  $D_1$ ,  $f, g$  be continuously differentiable functions from  $K$  to  $\mathbb{R}^{D_2}$ . If  $\xi$  is a reconfiguration map satisfies regularity condition A.5, then for every  $n \in \mathbb{N}$  there exists  $\theta_1^n, \dots, \theta_{N_n}^n$  in  $\Theta$  such that

$$\sup_{x \in K} \|f(x) - p \circ \mathbb{X}((x, g(x)) | \theta_1^n, \dots, \theta_n^n)\| < \frac{1}{n}.$$

Moreover, the limiting function  $\lim_{n \rightarrow \infty} p \circ \mathbb{X}((x, g(x)) | \theta_1^n, \dots, \theta_n^n)$  exists and is continuously differentiable  $K$ .

*Proof.* The proof will be deferred to the appendix.  $\square$

Non-Euclidean upgrading uses reconfigurations to improve a class of learning algorithms which we call objective learning algorithms. These are discussed in the next section.

## 2.2 Objective Learning Algorithms

The learning algorithms we consider in this paper optimize both the training set and validation set loss functions. Regularized regression, PCA, k-means, neural networks, Bayesian classifiers, support vector machines, and stochastic filters are all examples of objective learning algorithms.

Objective learning algorithms associate to every pair of training and validation sets of a given size, a pair of training set and validation set loss-functions as well as a pattern function linking the parameters being optimized to the prediction they can make. This formalization requires the definition of the set of all possible learning algorithms for a fixed set of hyper-parameters  $\Gamma$  and parameter to prediction function  $\phi : \mathbb{R}^d \times \mathbb{R}^D \rightarrow \mathbb{R}^{D \times k}$ . Here  $D$  is the dimension of the space in which the data-points lie,  $d$  is the dimension of the explanatory parameters, and  $k$  is the number of  $D$ -dimensional points out-putted by the algorithm.

For example, for a 1 factor PCA,  $k = 1$   $d = D$  and for a two factor PCA  $k = 2$  and  $d = D$ . In the case of linear regression, the regression weights are scalars therefore  $d = 1$ . If there is no intercept then  $k = 1$  and if there is an intercept  $k = 2$ , in this formulation  $D$  is the number of columns of the design matrix.

Let  $N_I$  be a positive integer and  $N_O$  be a non-negative integer. Define  $\Lambda_{\Gamma, \phi}^{N_I, N_O}$  to be the set of all pairs of maps  $(\mathcal{L}_I^{N_I}, \mathcal{L}_O^{N_O})$  such that

- (i) The map  $\mathcal{L}_I^{N_I} : \mathbb{R}^d \times C^\infty(\mathbb{R}^d \times \mathbb{R}^D, \mathbb{R}^{Dk}) \times \Gamma \times \mathbb{R}^{DN_I} \rightarrow [-\infty, \infty]$ ,
- (ii) The map  $\mathcal{L}_O^{N_O} : \mathbb{R}^d \times C^\infty(\mathbb{R}^d \times \mathbb{R}^D, \mathbb{R}^{Dk}) \times \Gamma \times \mathbb{R}^{DN_O} \rightarrow [-\infty, \infty]$ ,
- (iii) Regularity condition A.1 holds.

The function  $\phi(\beta|\cdot) : \mathbb{R}^D \rightarrow \mathbb{R}^{D \times k}$  represents the estimated pattern, parameterized by  $\beta$ . The parameter  $\beta$  lies in the space  $\mathbb{R}^d$  and is to be chosen by optimizing training set and validation set loss functions.  $\mathcal{L}_I^{N_I}$  is the training set loss function on a dataset of size  $N_I$  and  $\mathcal{L}_O^{N_O}$  is the out-of-sample loss function on a dataset of size  $N_O$ . The space of all learning algorithms for a specific pattern function  $\phi$  is  $\Lambda_{\Gamma, \phi} \triangleq \bigcup_{(N_I, N_O) \in \mathbb{N}^2} \Lambda_{\Gamma, \phi}^{N_I, N_O}$ .

**Definition 2.12** (Objective Learning Algorithm) *An objective learning algorithm is a map*

$$(\mathcal{L}_I, \mathcal{L}_O, \Gamma, \phi) : \bigcup_{(N_I, N_O) \in \mathbb{N}^2} \mathbb{R}^{D \times N_I} \times \mathbb{R}^{D \times N_O} \rightarrow \Lambda_{\Gamma, \phi},$$

$$(X^I, X^O) \mapsto \Lambda_{\Gamma, \phi}^{\frac{\text{Dim}(X^I)}{D}, \frac{\text{Dim}(X^O)}{D}},$$

where the pair of an training set and a validation set  $(X^I, X^O)$  are viewed as elements of  $\mathbb{R}^{D \times N_I} \times \mathbb{R}^{D \times N_O}$ , and where  $\text{Dim}(\cdot)$  is the non-negative integer-valued function mapping a point in Euclidean space to  $(\cdot)$ .

**Remark 2.13.** Given a dataset consisting of  $N$  data-points, the regression analysis loss function is

$$\sum_{i=1}^N (\beta^i X^i - Y^i), \quad (2.4)$$

where  $\{X^i\}_{i=1}^N$  are the data-points and  $\{Y^i\}_{i=1}^N$  are the responses. Incorporating an additional data-point  $X^{N+1}$  and an additional response  $Y^{N+1}$  into the regression analysis changes the loss function of Equation (2.4) to

$$\sum_{i=1}^{N+1} (\beta^i X^i - Y^i). \quad (2.5)$$

Both Equations (2.4) and (2.5) are a 1-dimensional regression problem but technically are defined by different loss functions. Definition 2.12 overcomes the oddity of having a learning algorithm differ depending on the size of the dataset, by defining an objective learning algorithm as a map associating the size of a dataset to the corresponding loss function; which is what we do in inadvertently.

Principal component analysis and regression analysis are objective learning algorithms. This is illustrated by the following two examples.

**Example 2.14** (Regression as an Objective Learning Algorithm). Let  $a < b$  be real numbers and  $\{f_i(x)\}_{i=1}^d$  be a continuously differentiable linearly independent set of functions in  $L^2([a, b])$ . Non-linear regression is an objective learning algorithm which is represented by

- (i)  $\phi(\beta|x) = \sum_{i=1}^d \beta_i f_i(x^i)$ ,
- (ii)  $\mathcal{L}_I^N(\beta, \phi(\beta|\cdot) | X_1^I, \dots, X_N^I) \triangleq \sum_{i=1}^N (y_i - \phi(\beta|X_i^I))^2$ ,
- (iii)  $\mathcal{L}_O^N(\beta, \phi(\beta|\cdot) | X_1^O, \dots, X_N^O) \triangleq \sum_{i=1}^N (y_i - \phi(\beta|X_i^O))^2$ ,
- (iv)  $\Gamma = \{0\}$ ,

where  $x^i$  is the  $i^{\text{th}}$  component of the  $D$ -dimensional vector  $x$  and where  $y_i$  is the  $i^{\text{th}}$  observed data-point. Typically, the out-of-sample dataset is always taken to be empty unless a regularization or sparsity constraint is imposed.

By adding a penalty term, such as the  $\ell^1$  norm, to the training set and validation set loss functions and expanding the hyperparameter set  $\Gamma$  accordingly, most regularized regression problems, such the LASSO of [31], are seen to be objective learning algorithms.



**Example 2.15** (PCA as an Objective Learning Algorithm). Calculating the first principal component of a dataset's empirical covariance matrix  $Q$  is an objective learning algorithm. Here  $(\mathcal{L}_I, \mathcal{L}_O, \Gamma, \phi)$  are represented by

- (i)  $\phi(\beta|x) = x\beta^T$ ,
- (ii)  $\mathcal{L}_I^N(\beta, \phi(\beta|X^I) | X_1^I, \dots, X_N^I) \triangleq - \left\{ \frac{\beta^T \tilde{X}_I^T \tilde{X}_I \beta}{\beta^T \beta} \right\}$ ,
- (iii)  $\mathcal{L}_O^N(\beta, \phi(\beta|X^O) | X_1^O, \dots, X_N^O) \triangleq - \left\{ \frac{\beta^T \tilde{X}_O^T \tilde{X}_O \beta}{\beta^T \beta} \right\}$ ,
- (iv)  $\Gamma = \{0\}$ ,

where  $\tilde{X}_I$  and  $\tilde{X}_O$  are the training and validation sets  $X^I$  and  $X^O$ , viewed as matrices but with their column-wise means removed. Typically, the out-of-sample dataset is always taken to be empty. The higher principal components, as well as sparse principal components, can also be represented analogously as an objective learning algorithm.

The optimal evaluation of a learning algorithm, is a map taking a learning algorithm and a dataset to an optimized pattern. The optimal evaluation is only well-defined on datasets which admit a unique optimizer. This set of regular datasets, called the regular domain of definition of the learning algorithm, is defined as follows.

**Definition 2.16** (Regular Domain of Definition) *Let  $(\mathcal{L}_I, \mathcal{L}_O, \Gamma, \phi)$  be a learning algorithm. The regular domain of definition of  $(\mathcal{L}_I, \mathcal{L}_O, \Gamma, \phi)$ , denoted by  $Dom(\mathcal{L}_I, \mathcal{L}_O, \Gamma, \phi)$ , is the set of all pairs of data points  $(X^I, X^O)$  in*

$$\bigcup_{(N_I, N_O) \in \mathbb{N}^2} \mathbb{R}^{D \cdot N_I} \times \mathbb{R}^{D \cdot N_O}$$

*satisfying the regularity condition A.2.*

The map associating a dataset and an objective learning algorithm to the pattern best describing it is now defined.

**Definition 2.17** (Optimal Evaluation) *Given an objective learning algorithm,  $(\mathcal{L}_I, \mathcal{L}_O, \Gamma, \phi)$  its optimal evaluation is the output of the function taking as input a pair training and validation sets in  $Dom(\mathcal{L}_I, \mathcal{L}_O, \Gamma, \phi)$  and returning the optimal parameter  $\beta(\hat{\gamma})$  defined by*

$$\hat{\gamma} \in \underset{\gamma \in \Gamma}{\operatorname{arginf}} \mathcal{L}_O^{N_O}(\beta(\gamma), \phi(\beta(\gamma)|X^O); \gamma | (X_1^O, \dots, X_{N_O}^O))$$

$$\beta(\gamma) = \underset{\beta \in \mathbb{R}^D}{\operatorname{arginf}} \mathcal{L}_I^{N_I}(\beta, \phi(\beta|X^I); \gamma | (X_1^I, \dots, X_{N_I}^I)).$$

**Remark 2.18.** The optimal evaluation takes an objective learning algorithm and a dataset and returns the optimizer minimizing the loss function defined by the dataset. For example, in a LASSO regression the optimal evaluation returns the parameters of the line of best fit relating the explanatory variables to the responses, with the tuning parameter is optimized according to the validation set.

The requirement that the dataset be in the regular domain of definition of the learning algorithm means that the optimal evaluation is a well-defined function. For example the points  $\{(1, 1), (-1, 1), (1, -1), (-1, -1)\}$  do not have a single line of best fit describing their relationship therefore the optimal evaluation of the regression problem is not defined on that dataset.

As in [14] the performance of a learning algorithm is defined as the negative of its loss function evaluated at the optimal value. The definition of performance of training and validation set performance of an objective learning algorithm is defined in an analogous manner.

**Definition 2.19** (Performance) *Let  $(\mathcal{L}_I, \mathcal{L}_O, \Gamma, \phi)$  be a learning algorithm. The training set performance of  $(\mathcal{L}_I, \mathcal{L}_O, \Gamma, \phi)$  is the function, denoted by  $\mathcal{P}^I(\mathcal{L}_I, \mathcal{L}_O)$ , taking a dataset  $(X^I, X^O)$  in  $\text{Dom}(\mathcal{L}_I, \mathcal{L}_O, \Gamma, \phi)$  to the extended real number*

$$\mathcal{P}^I(\mathcal{L}_I, \mathcal{L}_O) \left( \tilde{X}^I, \tilde{X}^O \right) \triangleq -\mathcal{L}_I^{N_I}(\beta(\hat{\gamma}), \phi(\beta(\hat{\gamma})); \hat{\gamma} \mid (X_1^I, \dots, X_{N_I}^I)).$$

*The validation set performance of  $(\mathcal{L}_I, \mathcal{L}_O, \Gamma, \phi)$  is the function, denoted by  $\mathcal{P}^O(\mathcal{L}_I, \mathcal{L}_O)$ , taking a dataset  $(X^I, X^O)$  in  $\text{Dom}(\mathcal{L}_I, \mathcal{L}_O, \Gamma, \phi)$  to the extended real number*

$$\mathcal{P}^O(\mathcal{L}_I, \mathcal{L}_O) \left( \tilde{X}^I, \tilde{X}^O \right) \triangleq -\mathcal{L}_O^{N_O}(\beta(\hat{\gamma}), \phi(\beta(\hat{\gamma})); \hat{\gamma} \mid (X_1^O, \dots, X_{N_O}^O)).$$

**Remark 2.20.** The performance is the negative of the loss function evaluated at its optimal evaluation. It provides a measure of how well an objective learning algorithm can explain a given dataset.

A dataset in  $\text{Dom}(\mathcal{L}_I, \mathcal{L}_O, \Gamma, \phi)$  is said to maximize the in (resp. out-of) sample performance of  $(\mathcal{L}_I, \mathcal{L}_O, \Gamma, \phi)$  if there is no other dataset in  $\text{Dom}(\mathcal{L}_I, \mathcal{L}_O, \Gamma, \phi)$  having the same number of training and validation data points and a higher validation set performance.

The main result can now be stated. If the data is in the regular domain of definition of a learning algorithm, and is not already in an optimal position, then there is a reconfiguration which increases the performance of that algorithm. An example of optimally positioned data for linear regression is data that is perfectly explained by a line both on the training and validation sets. In this extreme case, it is natural to expect that no improvement can be made to linear regression.

**Theorem 2.21** (Performance Gain). *Let  $D > 1$  and  $(\mathcal{L}_I, \mathcal{L}_O, \Gamma, \phi)$  be an objective learning algorithm. For every pair of integers  $N_I, N_O$  and every  $(X_I, X_O)$  in  $\text{Dom}(\mathcal{L}_I, \mathcal{L}_O, \Gamma, \phi)$ , there exists  $\theta_1^{N_I, N_O}, \dots, \theta_K^{N_I, N_O}$  in  $\Theta$  such that*

$$\mathcal{P}^O(\mathcal{L}_I, \mathcal{L}_O) \left( \tilde{X}^I, \tilde{X}^O \right) \geq \mathcal{P}^O(\mathcal{L}_I, \mathcal{L}_O) (X^I, X^O), \quad (2.6)$$

$$\mathcal{P}^I(\mathcal{L}_I, \mathcal{L}_O) \left( \tilde{X}^I, \tilde{X}^O \right) \geq \mathcal{P}^I(\mathcal{L}_I, \mathcal{L}_O) (X^I, X^O), \quad (2.7)$$

where the reconfigured datasets  $\tilde{X}^I$  and  $\tilde{X}^O$  are defined as

$$\begin{aligned} \tilde{X}_i^I &\triangleq \mathbb{X} \left( X_i^I \mid \theta_1^{N_I, N_O}, \dots, \theta_K^{N_I, N_O} \right), \\ \tilde{X}_i^O &\triangleq \mathbb{X} \left( X_i^O \mid \theta_1^{N_I, N_O}, \dots, \theta_K^{N_I, N_O} \right). \end{aligned}$$

The inequality in equation (2.7) (resp. equation (2.6)) is strict if  $(X_I, X_O)$  does not maximize  $\mathcal{P}^O(\mathcal{L}_I, \mathcal{L}_O)$  (resp.  $\mathcal{P}^I(\mathcal{L}_I, \mathcal{L}_O)$ ).

*Proof.* Without loss of generality assume that  $(X^I, X^O)$  does not maximize  $\mathcal{P}^O(\mathcal{L}_I, \mathcal{L}_O)$ , with the proof of the statement for  $\mathcal{P}^I(\mathcal{L}_I, \mathcal{L}_O)$  being identical. Therefore there is  $(\tilde{X}^I, \tilde{X}^O)$  in  $\text{Dom}(\mathcal{L}_I, \mathcal{L}_O, \Gamma, \phi)$  which has a higher value of  $\mathcal{P}^O(\mathcal{L}_I, \mathcal{L}_O)$  and has the same number of training and validation data-points.

Therefore, by the universal reconfiguration property of Theorem 2.9, there exists  $\theta_1^{N_I, N_O}, \dots, \theta_K^{N_I, N_O}$  such that  $\tilde{X}_i = \mathbb{X}(X_i | \theta_1^{N_I, N_O}, \dots, \theta_K^{N_I, N_O})$ .  $\square$

Theorem 2.21 guarantees that there exists a reconfiguration of the data which improves an algorithm's training set and validation set performance. The NEU meta-algorithm is a procedure which learns the reconfiguration of the space ensuring that the training and validation sets are positioned in a way which reduces the training set and validation set loss functions. This is formalized by the meta-algorithms illustrated by Figure 3 and made explicit in meta-algorithm 2.22.

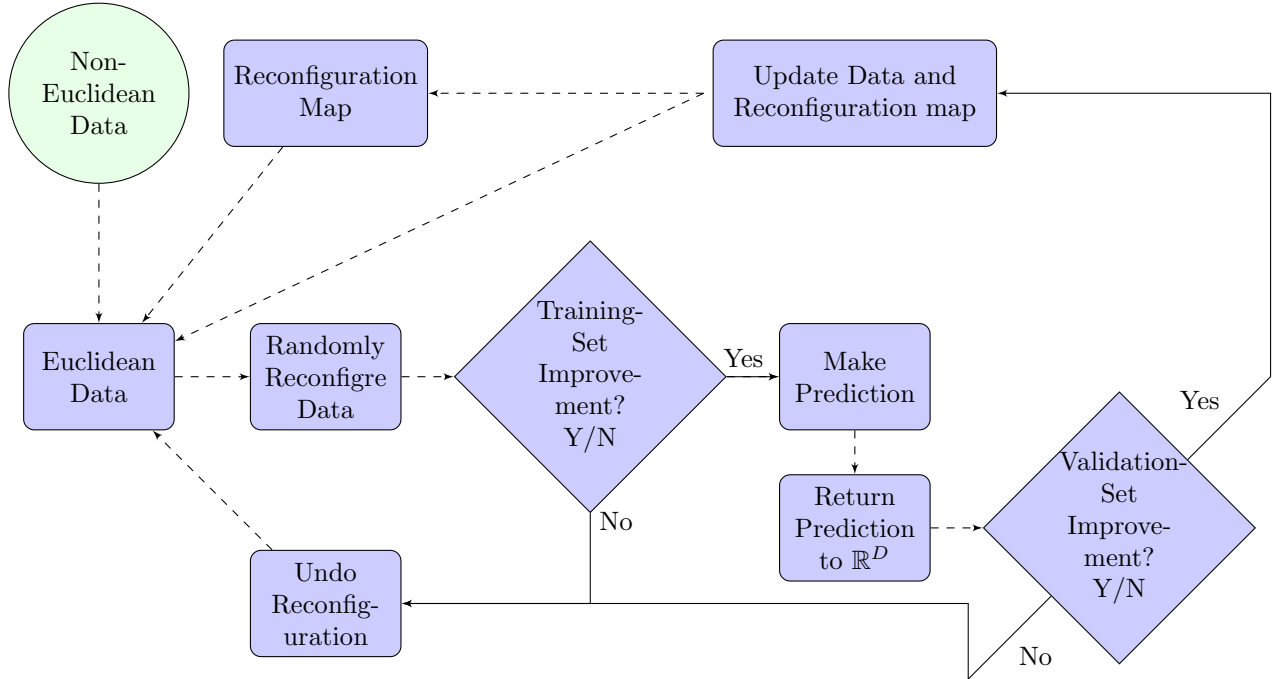


Figure 3: Work-flow of Reconfiguration Learning Phase of Non-Euclidean Upgrading

**Meta-Algorithm 2.22** (Non-Euclidean Upgrading). The inputs of the non-Euclidean upgrading algorithm are a diffeomorphism  $\Phi : \mathcal{M} \rightarrow \mathbb{R}^D$ , an objective learning algorithm  $(\mathcal{L}_I, \mathcal{L}_O, \Gamma, \phi)$ , a pair of training-set and validation-set data-points  $(\{X_i^I\}_{i=1}^{N_I}, \{X_i^O\}_{i=1}^{N_O})$  in  $\mathcal{M}$  satisfying regularity condition A.3,  $\mathbb{X}$  a reconfiguration map,  $\theta_0 \in \Theta_0$ ,  $\epsilon \in (0, 1]$ , and a positive integer  $N$ . Non-Euclidean upgrading takes these inputs and returns the following algorithms as its output

1. **Learning Reconfiguration:** Define a reconfiguration  $\mathbb{X}$  through the following procedure,

(a) Define the data-points  $X_i^{(0)} \triangleq \Phi(p_i)$ ,

(b)  $\theta^{(0)} \triangleq \theta_0$ ,

(c) For integers  $n$  between  $0 < n \leq N$ :

(i) Define the tentative optimal evaluation  $\beta^\uparrow(\hat{\gamma})$  to be

$$\hat{\gamma} \in \underset{\gamma \in \Gamma}{\operatorname{arginf}} \mathcal{L}_O^{N_O} \left( \beta^\uparrow(\gamma), \phi(\beta^\uparrow(\gamma)); \gamma \mid (\mathbb{X}(X_1^O \mid \theta), \dots, \mathbb{X}(X_{N_O}^O \mid \theta)) \right)$$

$$\left( \beta^\uparrow(\gamma), \theta(\gamma) \right) = \underset{\beta \in \mathbb{R}^D, \theta \in \Theta}{\operatorname{arginf}} \mathcal{L}_I^{N_I} \left( \beta, \phi(\beta); \gamma \mid (\mathbb{X}(X_1^I \mid \theta), \dots, \mathbb{X}(X_{N_I}^I \mid \theta)) \right),$$

(ii) Define the tentative performance measurement,  $\mathcal{P}^n(\mathcal{L}_I, \mathcal{L}_O)$  to be

$$\mathcal{P}^n(\mathcal{L}_I, \mathcal{L}_O) \triangleq \mathcal{P}^O(\mathcal{L}_I, \mathcal{L}_O) \left( \mathbb{X}(X_1^O \mid \theta), \dots, \mathbb{X}(X_{N_O}^O \mid \theta) \right),$$

(iii) **if**  $\mathcal{P}^n(\mathcal{L}_I, \mathcal{L}_O) > \mathcal{P}^{n-1}(\mathcal{L}_I, \mathcal{L}_O)$  **then**

| define  $\theta_1 \triangleq \theta(\hat{\gamma})$ .

else

| define  $\theta_n \triangleq \theta_0$ .

(iv) Define the updated data  $X_i^{(n)} \triangleq \xi \left( X_i^{(n-1)} \mid \theta_n \right)$ ,

(d) Stop when  $\frac{\mathcal{P}(\mathcal{L}_I, \mathcal{L}_O)}{\mathcal{P}^n(\mathcal{L}_I, \mathcal{L}_O)} < \epsilon$  or when  $n = N$ ,

(e) Define  $X_i \triangleq X_i^{(n)}$ ,

(f) Define the reconfiguration  $\mathbb{X} \triangleq \mathbb{X}(\cdot \mid \theta_1, \dots, \theta_N; \Phi)$ ,

2. **Perform Algorithm:** Perform  $(\mathcal{L}_I, \mathcal{L}_O, \Gamma, \phi)$  on the data  $(\mathbb{X}(X_i))_{i=1}^k$  and obtain the optimal evaluation  $\hat{X}$ ,

3. **Deconfigure Prediction:** Returns the values:

(a) **Prediction:**  $\mathbb{X}^{-1} \circ \phi(\hat{\beta} \mid \mathbb{X}(x))$ ,

(b) **Performance Gain:**  $\frac{\mathcal{P}^N(\mathcal{L}_I, \mathcal{L}_O)}{\mathcal{P}^0(\mathcal{L}_I, \mathcal{L}_O)}$ ,

(c) **Parameter Estimates:**  $\hat{\beta}$ .

Geometric and algebraic interpretations of NEU are discussed now, as well as connection to other geometric algorithms.

**Remark 2.23** (Geometric Interpretation). The reconfiguration  $\mathbb{X}$  is a diffeomorphism of  $\mathbb{R}^D$  back into itself. The pullback of the Euclidean metric  $d_E$  along  $\mathbb{X}$ , denoted by  $\mathbb{X}^*(d_E)$ , makes

$$(\mathbb{R}^D, \mathbb{X}^*(d_E)) = (\mathbb{X}(\mathbb{R}^D), \mathbb{X}^*(d_E)),$$

into a Riemannian manifold. The minimal distance curves in  $(\mathbb{R}^D, \mathbb{X}^*(d))$  are mapped to straight lines, through  $\mathbb{X}$ . Therefore the non-Euclidean algorithms in [11, 10, 13, 16] are all interpretable as parametric analogues to the NEU of PCA, regression, or Kalman filtering, but where the geometry is prespecified and not learned in an unsupervised manner.

**Remark 2.24** (Algebraic Interpretation). A smooth automorphism of  $\mathbb{R}^D$  is a smooth bijection from  $\mathbb{R}^D$  back onto itself, whose inverse is itself smooth. NEU is therefore a computational method for learning an autodiffeomorphisms which optimizes the validation-set and training set performance of a learning algorithm given a dataset.

In the next section, the numerical performance of NEU is investigated. The NEU algorithm is to improve regression analysis and principal component analysis and the resulting NEU-OLS and NEU-PCA algorithms are applied to financial time-series data.

### 3 Numerical Implementation of NEU-OLS and NEU-PCA

We begin by investigating the empirical performance of non-Euclidean upgrading. The first two implementations focus on real datasets and the second uses simulated data. The first two use the rapidly decreasing rotations to reconfigure the data whereas the last example uses micro-bumps since the data lies in  $\mathbb{R}^2$ .

#### 3.1 Data-driven Studies

The performance of the NEU meta-algorithm will be investigated both in the regression and dimensionality reduction settings on financial datasets beginning with a regression analysis study.

**Example 3.1** (Regression Analysis: Apple Stock Tracker). Predicting the relationship between the price of a set of assets is central to many trading strategies. For example, strategies that rely on illiquid assets may create a portfolio comprised entirely of liquid assets, which tracks the illiquid asset’s movements. Since that is a particular application of tracking portfolios, in this example, the technique is demonstrated using liquid stocks. The target stock price will be denoted by  $S_t$  and the prices of the assets making the tracking portfolio will be denoted by  $S_t^1, \dots, S_t^N$ .

In this example,  $S_t$  will be the price of apple stock, and  $S_t^1, \dots, S_t^N$  will be the stock prices for IBM, Google, Cisco Systems Inc., Microsoft Corporation, Acacia Communications Inc., NXP Semiconductors NV, Qualcomm, Analog Devices Inc., Glu Mobile Inc., Jabil Inc., Micron, and STMicroelectronics NV. These portfolio is chosen as being comprised of the stock of major companies in the same same industry as well as major companies making up apple’s supply chain (see [1] for a discussion on apple’s supply chain and [29] for a discussion of the 10 tech companies with the largest market capitalization).

A tracking portfolio consisting of these assets is built by minimizing the ordinary least-squares loss function on the training dataset

$$\sum_{i=1}^N \left( \left[ \frac{S_{t_i} - S_{t_{i-1}}}{S_{t_{i-1}}} \right] + \sum_{j=1}^d \beta_t^j \left[ \frac{S_{t_i}^j - S_{t_{i-1}}^j}{S_{t_{i-1}}^j} \right] \right)^2,$$

where  $N$  is the number of data points and  $d$  is the number of assets used to track the Apple stock price. For illustrative and comparative purposes, the LASSO of [31], the Ridge (or Tykhonov

regularization) regression of [32], the Elastic-Net regularization (ENET) of [34], and the NEU-OLS are compared.

The ENET selects the optimal regression weights by minimizing the loss function ENET Opt. Power denotes the solution to

$$\sum_{i=1}^N \left( \left[ \frac{S_{t_i} - S_{t_{i-1}}}{S_{t_{i-1}}} \right] + \sum_{j=1}^d \beta_t^j \left[ \frac{S_{t_i}^j - S_{t_{i-1}}^j}{S_{t_{i-1}}^j} \right] \right)^2 + \lambda \left[ (1 - \alpha) \sum_{j=1}^d |\beta^j| + \alpha \sum_{j=1}^d (\beta^j)^2 \right],$$

with  $\alpha, \lambda$  selected by sequential-validation. The LASSO is the special case where  $\alpha$  is fixed to 0 and Ridge regression is the special case where  $\alpha = 1$ . The penalty

$$\lambda \left[ (1 - \alpha) \sum_{j=1}^d |\beta^j| + \alpha \sum_{j=1}^d (\beta^j)^2 \right]$$

reduces the number of explanatory parameters in a model by forcing the regression weights towards 0, thereby forcing the most significant parameters to only be fit. The meta-parameter  $\lambda$  controls the strength of this sparsity penalty,  $\alpha \in [0, 1]$  controls the aggressiveness of the variable-selection process, with  $\alpha = 0$  giving a more aggressive choice and  $\alpha = 1$  towards a non-aggressive penalty. ENET, LASSO, and Ridge regression are interpreted in [33] as robust regression problems where the regression problem is optimized against varying types of shocks in the data, or alternatively these can be interpreted as in [31, 35] as modifications of the regression problem that are able to detect and converge to the true set of explanatory variables, under linear and Gaussian noise assumptions.

In this example, 2 years of adjusted stock prices are used to compute the weights, ending on July 25<sup>th</sup> 2018. The modeling assumption that the data does not follow a constant pattern throughout time is made and the data is broken up into rolling windows. Regression weights are dynamically updated on each window as is standard in practice (for example see [9, 2, 30]). In order to extract meaningful weights  $\beta_t^1, \dots, \beta_t^N$ , the time-series must be shown to be co-integrated. The Dickey-Fuller, unit root test is performed on the returns of the adjusted stock price time-series and the null-hypothesis that there exists a unit root is rejected with a p-value of less than .01 and Dickey-Fuller statistic  $-2.8453$ , therefore the  $\beta_t$  can meaningfully be computed from the adjusted stock price's returns using regression methods (see [22] for more details on co-integrated time-series).

	Mean	95 L	95 U	99 L	99 U
OLS	4.185	4.038	4.385	4.017	4.448
Ridge	-0.831	-0.916	-0.715	-0.928	-0.678
LASSO	0.581	0.568	0.599	0.566	0.604
ENET	0.526	0.519	0.535	0.518	0.538
NEU-OLS	0.204	0.202	0.208	0.202	0.209

Table 1: Mean Aggregate Training Errors.

Each window is sequentially divided into a training, a validation, and a test set. Each of the training sets consists of 200 observations, the validation sets consist of 2 weeks, and the test

sets consists of the last week of each moving window. The proportions invested in each asset, denoted are the regression weights on that window, and are recalibrate on each window using each of the stocks' returns. The mean training, validation, and test errors aggregated across each windows are reported in the Tables 1, 3, and 2, respectively. The optimal parameters for the Ridge, LASSO, ELASTIC-NET, and NEU-OLS are re-calibrated on every window using sequential validation. The optimization of the parameters defining the reconfiguration of the data on were performed by alternating between stochastic gradient descent and randomized searches of the parameter space.

	Mean	95%L	95%U	99%L	99%U
OLS	4.217	4.214	4.222	4.214	4.224
Ridge	-0.853	-0.946	-0.726	-0.959	-0.686
LASSO	0.582	0.573	0.594	0.572	0.598
ENET	0.525	0.518	0.534	0.517	0.537
NEU-OLS	0.204	0.203	0.206	0.203	0.206

Table 2: Mean Aggregate Testing Errors.

	Mean	95%L	95%U	99%L	99%U
OLS	4.202	4.058	4.397	4.038	4.458
Ridge	-0.845	-0.928	-0.734	-0.939	-0.699
LASSO	0.581	0.571	0.594	0.569	0.598
ENET	0.525	0.521	0.530	0.520	0.531
NEU-OLS	0.204	0.203	0.206	0.202	0.206

Table 3: Mean Aggregate Validation Errors.

As expected the OLS performs worst and the ENET performs best amongst the benchmark regression methods. All the methods, except the Ridge regression are conservative and underestimate the price of apple stock. The NEU-OLS has the lowest error in the training, validation, and test sets across every window. Moreover, it has the tightest confidence intervals. Therefore the NEU-OLS performs achieves a lower bias as well as a lower variance.

Algorithm	OLS	NEU-OLS	Ridge	LASSO	ENET
Run Time (sec)	0.01	104.02	0.02	0.02	0.07
$\frac{\text{Run Time}}{\text{Run Time OLS}}$	1	12,980.03	2.74	2.57	9.11

Table 4: Runtime Comparison.

The NEU-OLS does have its own drawbacks, namely computational time. Once the reconfiguration of the data is learned the OLS algorithm can be run directly on the reconfigured dataset making NEU-OLS and OLS just as fast. However on the first run, when the reconfiguration is being learned the NEU-OLS is significantly slower than the other methods compared within this paper.

Table 4 reports the run-times of performing the OLS, NEU-OLS, Ridge regression, LASSO, and ENET algorithms on the dataset considered in this example using an Intel(R) Core(TM)

i5-6200U CPU at 2.30GHz, with 7844MB available RAM machine running 18.04 LTS version of the Ubuntu Linux distribution.

We conclude that after learning the NEU-OLS has the lowest prediction error amongst the regression methods considered in this example and its execution speed is just as fast as OLS after the reconfiguration has been learned. However, on the first run when the reconfiguration is being learned NEU-OLS is notably slower than the other methods. Therefore, NEU-OLS may be the best of these options when speed is not a large factor, but it may not be ideal for setting when the runtime of an algorithm is a determining factor, such as for live high-frequency trading.

**Example 3.2** (Dimensionality Reduction: German-Bond Yield Curve). Principal component analysis (PCA) is a non-parametric technique which converts correlated data  $\{x_1, \dots, x_N\}$  into a set of uncorrelated vectors  $v_{(1)}, \dots, v_{(K)}$ , each explaining progressively less of the data's variance than the last one. The vectors  $\{v_{(k)}\}_{k=1}^K$ , called principal components, are obtained through the recursion relation:

$$\begin{aligned}\hat{\mathbf{Q}}_k &\triangleq \mathbf{Q} - \sum_{s=1}^{k-1} \mathbf{Q} \mathbf{x}_{(s)} v_{(s)}^T \\ v_{(k)} &\triangleq \arg \max_{\|v\|=1} \left\{ \|\hat{\mathbf{Q}}_k v\|^2 \right\} \\ v_{(0)} &\triangleq 0.\end{aligned}\tag{3.1}$$

where  $\mathbf{Q}$  is the empirical data matrix with column-wise means removed.

PCA is commonly used in finance, where high dimensional data is typical. A classical use is for pricing zero-coupon bonds. Denote by  $B(t, T)$  the price of a zero-coupon bond with maturity  $T$  at time  $t$ . The price  $B(t, T)$  can be modeled using the yield curve  $y(t, T)$ , which is defined as the rate at which the price of the bond is equal to the discounted cash flows. That is,

$$y(t, T) \triangleq \ln \left( \frac{B(t, T)}{T - t} \right).$$

The first three principal components of the yield curve are known to explain its level, slope, and curvature respectively (see [7] for more details). The validation-set loss function which we will use is

$$\min_{\beta_1, \dots, \beta_k \in \mathbb{R}^{\tilde{K}}} \sum_{i=1}^n \left( Y_i - \sum_{k=1}^{\tilde{K}} \beta_k v_{(k)} \right)^2,\tag{3.2}$$

where  $Y_i$  is the vector of Bond yields observed on the  $i^{\text{th}}$  day in the validation set (resp. training set) and  $\tilde{K} \leq K$  is the number of principal components used to give a low dimensional approximation of the yield curve. As discussed in [7], the first three principal components  $v_{(1)}, v_{(2)}, v_{(3)}$  of most yield curves tend to explain about 95% of the data's variance.

As a benchmark a two common alternatives to PCA, Kernel PCA (kPCA) and sparse PCA (sPCA) will be also be considered. Kernel PCA, performs first maps the data into another space, called the feature space, wherein the data can be more naturally partitioned by hyperplanes and the performs PCA in the feature space. The transformation into the feature space is typically made indirect by only describing the feature space's inner product, which is possible due to



the reproducing kernel Hilbert space structure of the feature space. A choice of inner product between two vectors  $v_1, v_2$  in the feature space is

$$K \triangleq \left( e^{\frac{-\|x_i - x_j\|^2}{2\sigma^2}} \right)_{i,j=1}^N.$$

Unlike NEU-PCA, the non-linear transformation used in kPCA is not learned from the data but chosen before the algorithm is executed. Since kPCA does not make computations directly in the feature space but works indirectly to it by exploiting its inner product, kPCA does not allow for reconstruction of the data. However this is not the case with NEU-PCA, since it is entirely constructive.

Analogously to the LASSO, Ridge regression, and ENET regularization problems, sPCA penalizes the Equation (3.1) to in order to obtain sparser principal components. The implementation considered in this paper will use the sPCA formulation of [8]. Sparse PCA has the advantage over PCA of being more interpretable, lower-dimensional, and being more robust due to its low dimensionality (see [36, 8] for more details on sPCA).

For this illustration PCA, kPCA, sPCA, NEU-PCA, NEU-kPCA, and NEU-sPCA will all be performed on bond yield data. The daily bond data considered in this example consists of stripped German government bond prices between January 4<sup>th</sup> 2010 and December 30<sup>th</sup> 2014. The considered bond maturities are between 6 months and 30 years. The training-set consists of the first 1000 days of data, the validation set of the next 200 days, and the test set consists of the remainder. The reconfigurations defining the NEU methods will be learned using NEU-PCA. The NEU-kPCA and NEU-sPCA methods will be use the reconfigurations learned from NEU-PCA.

The NEU-PCA algorithm is implemented by optimized the training and validation objective functions by alternating between random searches and performing bulk iterations of the Nelder-Mead heuristic search method (see [21] for details Nelder-Mead optimization). This heuristic scheme provided faster convergence results than direct use of stochastic gradient descent as in Example 2.14 due to the data’s high dimensionality. After learning the reconfigurations defining the NEU-PCA algorithm, the same reconfigurations were used to define NEU-kPCA and NEU-sPCA. This is interpreted as a form of transfer learning between analogous models.

N. Fact.	PCA	NEU-PCA	kPCA	NEU-kPCA	sPCA	NEU-sPCA
1	0.7749	0.7868	0.0906	0.0894	0.9756	0.9774
2	0.8833	0.8936	0.9171	0.9175	0.9942	0.9949
3	0.9417	0.9506	0.9948	0.9955	0.9992	0.9996
4	0.9654	0.9688	0.9981	0.9981	0.9999	0.9999

Table 5: Comparison of Variance Explained in Training Set.

Table 5 shows that NEU-PCA explains more of the training set variance than PCA does. However, kPCA and sPCA seem to explain more training set variance than NEU-PCA, but not as much as NEU-kPCA or NEU-sPCA. However, examining the test-set predictive performance

of the four algorithms in Table 6, it is observed that the kPCA based algorithms are not able to accurately forecast the yield curve. Therefore, NEU-PCA is the most parsimonious option for prediction between the four methods and NEU-kPCA explains the most training set variance of the data.

The more modest gains of this method are due to the district training and validation loss functions. For example, removing the validation loss-function and thereby the early stopping criterion in the definition of NEU, it can be seen that one NEU-PCA can explain more than 99.99% of the training set variability of the data. However, this leads to poor out-of-sample predictions of the test set yield curves as well as uninterpretable NEU-PCAs.

N.Fact.	PCA	NEU-PCA	kPCA	NEU-kPCA	sPCA	NEU-sPCA
1	2,245.643	2,153.412	829.210	827.651	497.683	471.695
2	344.961	294.106	829.200	827.644	290.040	265.822
3	28.633	17.927	829.197	827.640	14.489	12.400
4	4.424	2.975	829.190	827.634	12.061	12.210

Table 6: Comparison of test set Predictions according to the loss-function of Equation (3.2).

In this implementation, the NEU-PCAs of the yield curve. Figure 4 shows that, upon rescaling, the first and fourth PCA and NEU-PCAs have identical interpretation, while the second and fourth NEU-PCAs look similar a flipped version of the second and fourth PCAs. The NEU-PCAs in Figure 4 are in the transformed, non-Euclidean space, whereas the PCAs in Figure 4 are in Euclidean space itself. It should not be surprising that the 1 and 4 factor sPCA outperforms the 1-factor NEU-sPCA since the reconfiguration used for the NEU-sPCA was trained using the PCA algorithm.

In this implementation, the NEU-PCAs provided the most robust out-of-sample predictions of the yield curve, explained more of the training set variance than PCAs did and retained the interoperability of each of the principal components. Moreover like PCA, the approach is constructive therefore can be used for reconstruction purposes, which is not the case for kPCA due to it indirectly working with the feature space (see [27, Section 4] for a brief discussion on the data-reconstruction shortcomings of kPCA).

Table 7 examines the runtime of each method. All six algorithms were run on a machine with the same specs as those of Example 2.14.

Algorithm	Run Time (sec)	$\frac{\text{Run Time}}{\text{Run Time PCA}}$
PCA	0.01	1
NEU-PCA	2.89	474.99
kPCA	0.08	12.50
NEU-kPCA	2.96	486.48
sPCA	0.81	132.40
NEU-sPCA	3.70	606.39

Table 7: Runtime Comparison.

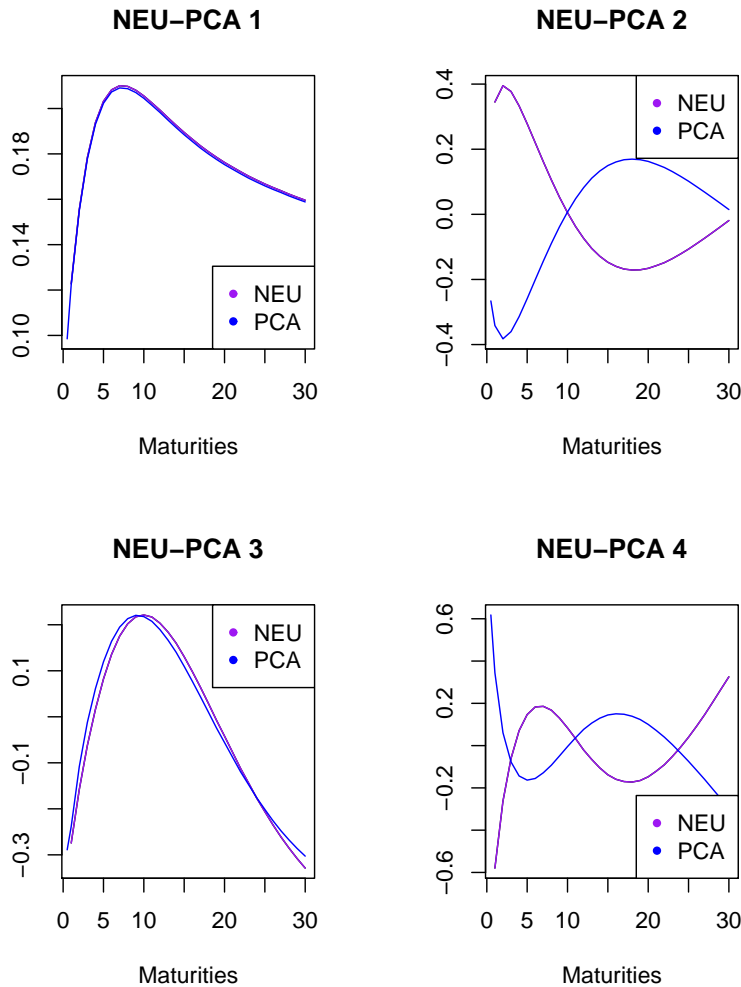


Figure 4: First four principal components of the German Bond Yield-curve.

The central shortcoming of the NEU meta-algorithm is underlined by Table 7. Its second row shows that the runtime of the NEU algorithms are about 1000 times slower than PCA and 100 times slower than kPCA. Therefore if speed is necessary it may be more desirable to turn to PCA or kPCA than their NEU counterparts. However, if time can be spared then the first three NEU-PCAs makes 3-factors NEU-PCA the best overall choice due to its interpretability, out-of-sample predictive power and it explaining a competitive level of the training set's variance.

The next example investigates the implications of the universal approximation and universal reconfiguration properties of reconfigurations in the controlled environment provided by simulation studies.

### 3.2 Simulation Studies - Investigation of Universal Properties

These simulation studies will focus on the illustrating the universal approximation and universal reconfiguration properties of reconfigurations, and thus the NEU meta-algorithms through the lens of regression analysis. In these simulation studies, the data will be generated according to the model

$$y = m(x) + \sigma\epsilon, \quad (3.3)$$

where  $\epsilon \sim N(0, 1)$ ,  $\sigma > 0$ , and  $m$  is a non-linear function. Three non-linear functions will be investigated, these are

1.  $\min(e^{-\frac{1}{(x+1)^2}}, x + \cos(x))$ ,
2.  $\cos(e^{-x})$ ,
3.  $I(x < 0.5)$

The first function investigates how well NEU-OLS can approximate non-linear functions whose global shape, unlike polynomials or periodic function, cannot be determined by local data. The second evaluates how NEU-OLS can deal with functions osculating at non-constant speeds. The third looks at how well the NEU-OLS algorithm can approximate functions with discontinuities.

The NEU-OLS algorithm will be benchmarked against two standard non-parametric regression algorithms, penalized smoothing splines regression (p-splines) and Locally Weighted Scatterplot Smoothing (LOESS). Smoothing splines regression is a highly flexible approximation method. A smoothing splines is a twice continuously differentiable function which is constructed by gluing a finite number  $k$ , at most equal to  $n$ , of cubic polynomials together. The optimal p-spline, denoted here by  $g$ , is chosen by minimizing the objective function

$$\sum_{i=1}^n (y_i - g(x_i))^2 + \lambda \int \frac{\partial^2 g}{dx}(x)^2 dx,$$

where  $x_i$  are real numbers,  $f$  is a suitable function,  $\lambda \geq 0$ , and the pairs  $(x_i, y_i)$  are generated according to the model described in Equation (3.3).

The value of the tuning parameter  $\lambda$  determines how smooth  $g$  is and how well it interpolates the data-points  $\{(x_i, y_i)\}_{i=1}^n$ . If  $\lambda = 0$  and  $k = n$ , then  $f$  interpolates the data. Conversely, as  $\lambda$  approaches infinity and  $k$  becomes small, then  $g$  approaches the solution to an ordinary linear regression (see [14, Chapter 5] for details on smoothing splines and p-splines). Unlike smoothing splines, p-splines do not require a knot at every point and therefore are less susceptible to over-fitting than smoothing splines. The parameters  $k$  and  $\lambda$  will be chosen by 4-fold cross-validation.

LOESS is a non-parametric regression method, where a smooth polynomial is fit to the data. The best fitting polynomial, denoted by  $g$ , is found by minimizing the value of the loss-function

$$\sum_{i=1}^n w(x_i) (y_i - g(x_i)),$$

$$w(x) \triangleq (1 - |d|^3)^3,$$

where  $d$  is the distance of the point  $x$  to the polynomial. Unlike classical regression problems, the LOESS objective function does not only look at the pairs  $(x_i, y_i)$  themselves but incorporates the importance of nearby points into its objective function. This is because the closest point on  $g$  to  $x$  need not be  $g(x)$  but may be a neighboring point on  $g$  to  $g(x)$ . The degree of the polynomial is chosen using cross-validation (see [4] for details).

For each simulation  $10^3$  observations will be generated on the interval  $[-3, 3]$ , the data will then be normalized to the unit square for uniformity between the three examples. The models' tuning-parameters will be estimated on a subset of 100 data-points sampled in a stratified manner on 5 evenly spaced subintervals by cross-validation or early stopping in the case of NEU-OLS. The remaining sample points will serve as the test set. The run-times reported in these simulation studies will be using the same specs as the PC used to report the run-times in Table 4.

**Example 3.3** (Simulation Study - NEU-OLS - Non-Locality). In this simulation study, NEU-OLS will be compared against LOESS and  $p$ -splines regression when the function  $m$  in Equation (3.3) is assume to be

$$m(x) = \min(e^{-\frac{1}{(x+1)^2}}, x + \cos(x)). \quad (3.4)$$

This simulation study was performed by generating 1,000 i.i.d. samples from the model of equation (3.4).

The optimal smoothing parameter for the  $p$ -splines was found to be  $\lambda = 0.976$ . The parameter  $\lambda$  was learned using 4-fold cross-validation. In Table 8, the estimated test-set mean squared error for predicting  $y$  are reported in the first table for various values of  $\sigma$ . NEU-OLS outperforms the other models has a lower estimated test-set mean squared error, with the exception of  $p$ -splines regression when  $\sigma = 1.5$ . This is likely due to the low robustness of OLS to high amounts of noise as compared to penalized methods (see [33] for an interpretation of penalized regression methods as robust regressions).

$\sigma$	NEU-OLS	p-Splines	LOESS
0.1	5.53e-04	3.11e-03	3.04e-03
0.3	1.26e-03	6.30e-03	1.22e-02
0.5	4.82e-03	1.45e-02	2.49e-02
1.5	6.81e-02	5.92e-02	8.03e-02

Table 8: Estimated Test-Set Mean Squared Errors.

The non-parametric 95%-confidence intervals in Table 9 are computed using the bootstrap adjusted confidence (BAC) interval method of [6]. The BAC method is chosen since it does not assume that the underlying distribution is Gaussian, it corrects for bias, and it corrects for skewness in the data. The bootstrapping was performed by re-sampling 1,000 times from the realized error distributions.

Table 9 illustrates that NEU-OLS has tighter confidence intervals for its mean error as well as a mean error which is closer to 0 for each of the values of  $\sigma$  reported here. This is likely due to the flexibility of NEU-OLS and therefore its ability to capture complicated patterns in the data, as is expected from Theorem 2.9. The discrepancy between the cases lower mean error and

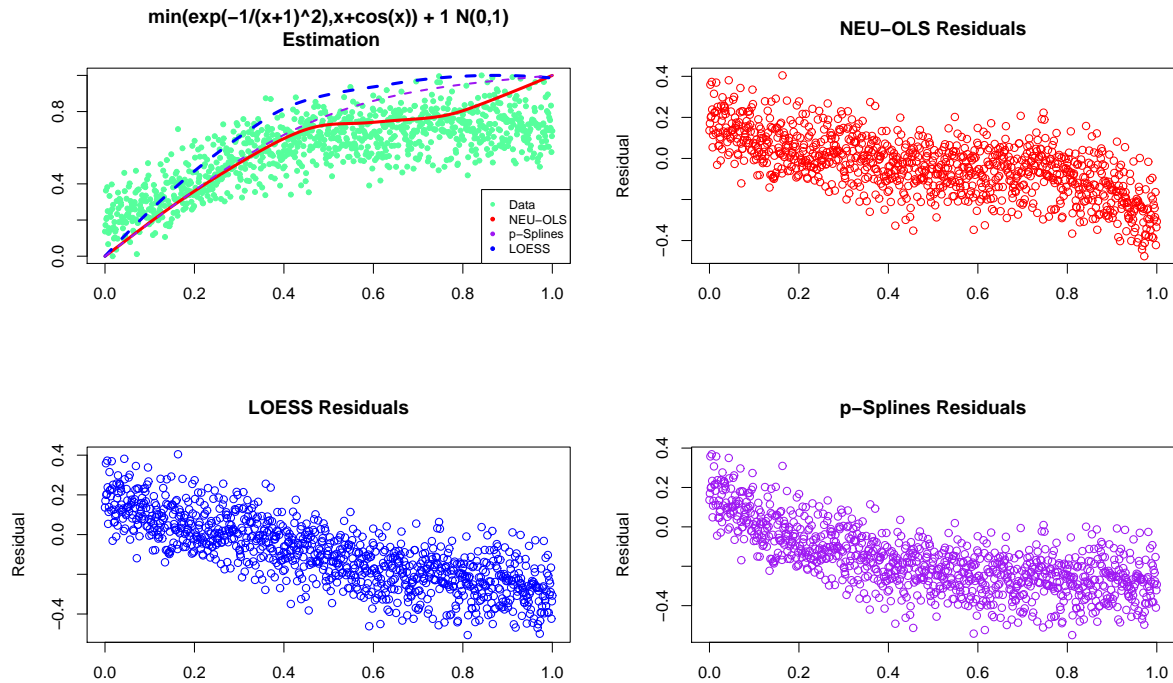


Figure 5: Estimation of  $\min(e^{\frac{-1}{(1+x)^2}}, x + \cos(x))$  using various methods.

higher estimated test-set mean squared error when comparing NEU-OLS and p-splines when  $\sigma = 1.5$  is due to the oscillatory behavior of the NEU-OLS curve.

$\sigma$	NEU-OLS	p-Splines	Loc-Reg
0.1	1.09e+01	1.29e-02	8.39e-02
0.3	8.14e+00	1.33e-02	8.22e-02
0.5	5.20e+00	1.81e-02	9.95e-02
1.5	4.18e+00	1.68e-02	7.77e-02

Table 10: Runtime Metrics in seconds.

Table 10 shows that the runtime of NEU-OLS scales with noise, more so than the other algorithms. This can be interpreted as NEU-OLS learning the patterns in the data and having to reject more tentative reconfigurations which have been fit to test-set noise, after testing them on the validation set. In each of these cases, NEU-OLS is notably slower than the other two algorithms.

The increase in speed between the cases where  $\sigma = 0.5$  and  $\sigma = 1.5$  is due to the early stopping criteria in Algorithm 2.22 (1.d). This is because the function  $m$  becomes increasingly difficult to differentiate from the noise  $\epsilon$  as  $\sigma$  becomes larger, leading the NEU meta-algorithm to terminate just before noise becomes mixed into the estimate for  $m$ .

$\sigma = 0.1$	95 L	Mean	95 U
NEU-OLS	3.78e-03	5.13e-03	6.47e-03
p-Splines	2.53e-02	2.83e-02	3.14e-02
LOESS	-5.03e-02	-4.86e-02	-4.71e-02
$\sigma = 0.3$	95 L	Mean	95 U
NEU-OLS	-5.90e-03	-3.90e-03	-1.67e-03
p-Splines	-1.68e-02	-1.22e-02	-7.40e-03
LOESS	-9.30e-02	-8.91e-02	-8.48e-02
$\sigma = 0.5$	95 L	Mean	95 U
NEU-OLS	-3.82e-02	-3.49e-02	-3.09e-02
p-Splines	-4.97e-02	-4.30e-02	-3.63e-02
LOESS	-1.26e-01	-1.20e-01	-1.13e-01
$\sigma = 1.5$	95 L	Mean	95 U
NEU-OLS	-1.33e-01	-1.18e-01	-1.05e-01
p-Splines	-1.34e-01	-1.21e-01	-1.09e-01
LOESS	-2.10e-01	-1.98e-01	-1.85e-01

Table 9: Estimates of Confidence Intervals of mean errors.

**Example 3.4** (Simulation Study - NEU-Regression - Osculating Functions). In this simulation study the function  $m$  in Equation (3.3) is

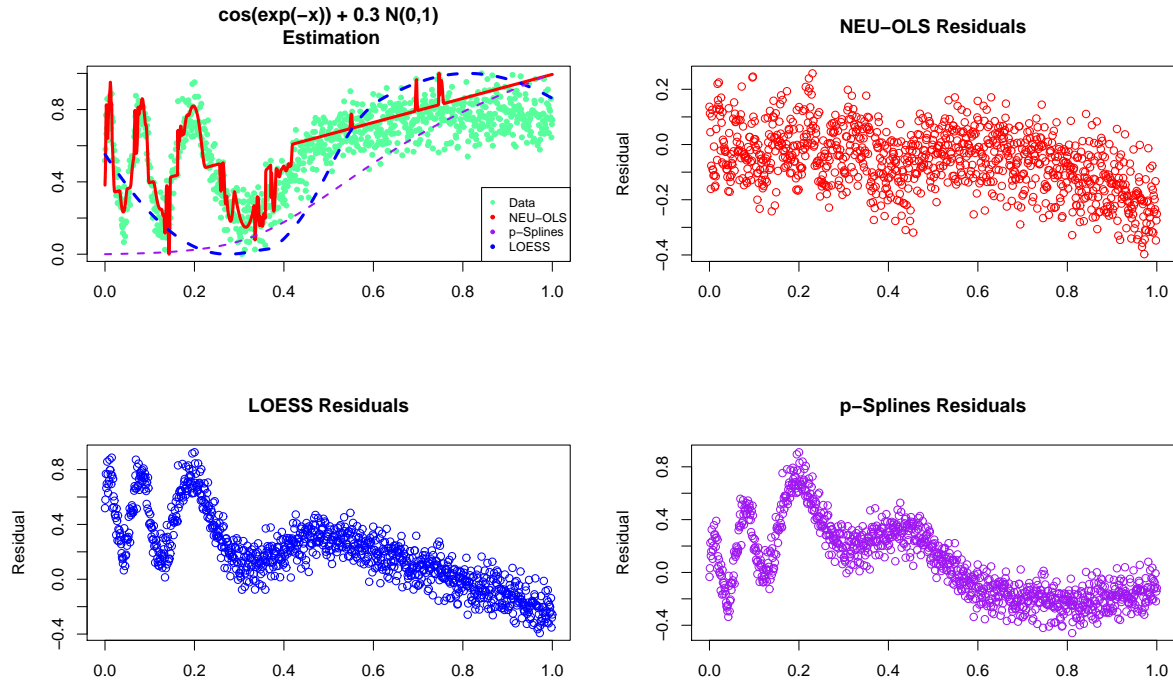
$$m(x) = \cos(e^{-x}).$$

Figure 6 illustrates that all three methods have difficulty capturing the osculations. However, the NEU-OLS comes the closest to capturing the shape of the function  $m$ . However, looking at the residuals plots of the same figure NEU-OLS is seen to be a more appropriate non-parametric regression algorithm.

$\sigma$	NEU-OLS	p-Splines	LOESS
0.1	3.66e-03	1.30e-01	7.96e-02
0.3	1.65e-02	1.08e-01	8.39e-02
0.5	2.09e-02	1.06e-01	9.66e-02
1	1.16e-01	1.18e-01	1.22e-01

Table 11: Estimated Mean Squared Error from data.

Tables 11 and 12 illustrate that the NEU-OLS algorithm is better at estimating  $y$  from the noisy observations, generated according to Equation (3.3), than the other two algorithms. The performance gap between the methods begins to close as  $\sigma$  is increased. This is most likely due to the oscillatory behavior of the function  $m$  and the noise becoming increasingly difficult to be distinguished between when learning the reconfigurations.

Figure 6: Estimation of  $\cos(\exp(-x))$  using various methods.

$\sigma = 0.1$	95 L	Mean	95 U
NEU-OLS	1.99e-02	2.33e-02	2.69e-02
p-Splines	2.45e-01	2.60e-01	2.76e-01
LOESS	1.13e-01	1.27e-01	1.44e-01
$\sigma = 0.3$	95 L	Mean	95 U
NEU-OLS	-4.54e-02	-3.82e-02	-3.00e-02
p-Splines	1.83e-01	1.99e-01	2.15e-01
LOESS	5.12e-02	6.79e-02	8.68e-02
$\sigma = 0.5$	95 L	Mean	95 U
NEU-OLS	-5.05e-02	-4.19e-02	-3.24e-02
p-Splines	1.47e-01	1.64e-01	1.82e-01
LOESS	1.71e-02	3.51e-02	5.59e-02
$\sigma = 1$	95 L	Mean	95 U
NEU-OLS	-1.89e-01	-1.73e-01	-1.54e-01
p-Splines	1.12e-01	1.31e-01	1.51e-01
LOESS	-1.27e-02	6.90e-03	3.09e-02

Table 12: Estimates of Confidence Intervals for Estimated Test-Set Errors.

The high amount of oscillation in  $m(x)$  makes noise difficult to differentiate from the value of  $m(x)$  for the  $p$ -Splines and LOESS methods as is reflected in the residual plots in Figure 6.



However, the flexibility of NEU-OLS is able to surmount this issue but does result in a bump curve. Similarly to Table 9, Table 12 confirms the lower estimated test-set errors and tighter confidence intervals of the NEU-OLS algorithm as compare to  $p$ -splines and LOESS. The longer

$\sigma$	NEU-OLS	p-Splines	LOESS
0.1	4.63e+00	1.47e-02	8.54e-02
0.3	4.55e+00	1.51e-02	8.58e-02
0.5	4.57e+00	1.72e-02	8.82e-02
1	4.56e+00	1.38e-02	8.31e-02

Table 13: Runtime Metrics

run-time of the NEU-OLS algorithm, reported in Table 13 is not much of a shortcoming as it was in Example 3.3 due to the large performance gain it provides when estimating osculating functions as was seen in Table 11.

The next and final example explores a situation which is beyond the comfortable ability of all three of the proposed methods. Nevertheless, NEU-OLS best handles this next estimation problem.

**Example 3.5** (Simulation Study - Discontinuities). The function  $m$  in Equation (3.3) will be

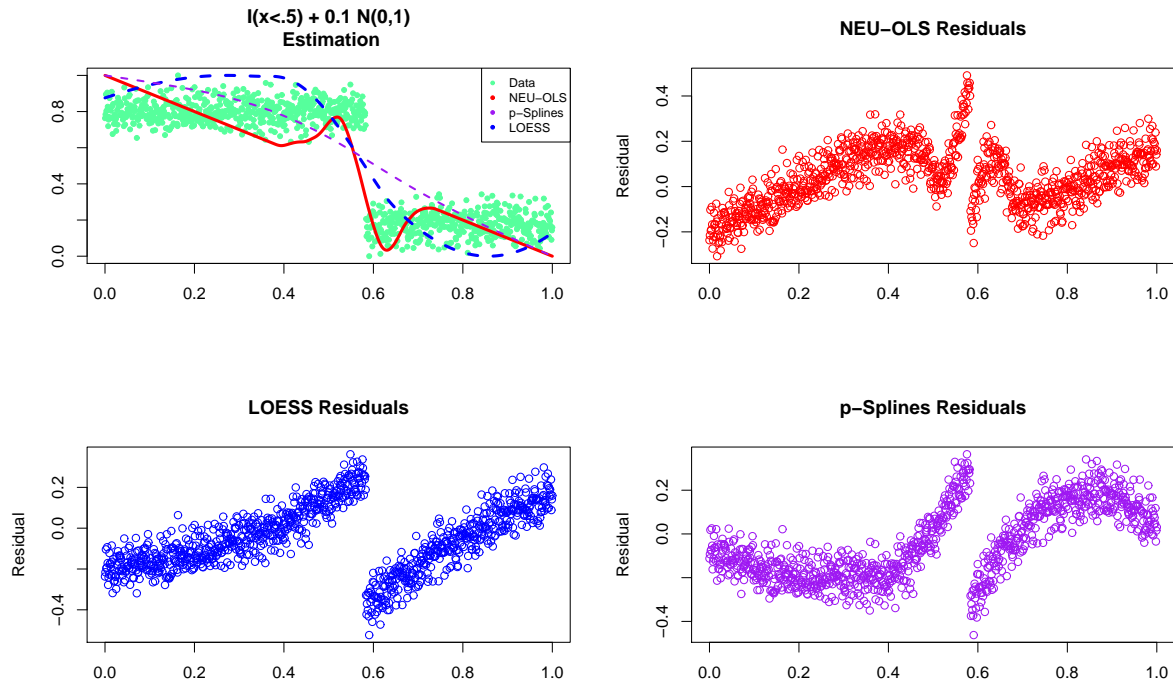
$$m(x) = I(x < .5),$$

for this last simulation study investigating how well NEU-OLS captures jump discontinuities. Each of the residual plots in Figure 7 show that all three methods have difficulty with the stark discontinuity. However the plot does seem to indicate that NEU-OLS can better handle this jump, the is likely due to the locality property of reconfigurations. Table 14 the NEU-OLS

$\sigma$	NEU-OLS	p-Splines	LOESS
0.1	1.84e-02	2.71e-02	2.90e-02
0.3	3.88e-02	5.06e-02	7.93e-02
0.5	5.81e-02	7.11e-02	1.10e-01
1	8.38e-02	9.78e-02	1.44e-01

Table 14: Estimated Test-Set Mean Squared Errors.

Tables 14 and 15 show that NEU-OLS performs best when estimating the function  $m$ . However, the graph in Figure 7 shows that NEU-OLS best captures the shape of the indicator function  $I(x < \frac{1}{2})$ .

Figure 7: Estimation of  $I(x < \frac{1}{2})$  using various non-parametric regression methods.

$\sigma = 0.1$	95 L	Mean	95 U
NEU-OLS	3.35e-02	4.08e-02	4.93e-02
p-Splines	-5.89e-02	-4.96e-02	-4.04e-02
LOESS	-5.25e-02	-4.18e-02	-3.13e-02
$\sigma = 0.3$	95 L	Mean	95 U
NEU-OLS	-2.72e-03	9.77e-03	2.11e-02
p-Splines	-9.28e-02	-8.02e-02	-6.70e-02
LOESS	-8.68e-02	-6.95e-02	-5.22e-02
$\sigma = 0.5$	95 L	Mean	95 U
NEU-OLS	-1.78e-02	-2.62e-03	1.16e-02
p-Splines	-1.07e-01	-9.21e-02	-7.68e-02
LOESS	-9.79e-02	-7.78e-02	-5.62e-02
$\sigma = 1$	95 L	Mean	95 U
NEU-OLS	-3.30e-02	-1.50e-02	2.12e-03
p-Splines	-1.22e-01	-1.03e-01	-8.53e-02
LOESS	-1.00e-01	-7.73e-02	-5.24e-02

Table 15: Estimates of Confidence Intervals for Mean Test-Set Errors.

All three simulation studies show that NEU-OLS is competitive with two standard non-parametric regression procedures. Moreover, it better handles discontinuities, oscillatory be-

$\sigma$	NEU-OLS	p-Splines	LOESS
0.1	5.60e+00	1.08e-01	9.07e-02
0.3	4.69e+00	1.90e-02	1.10e-01
0.5	5.21e+00	1.75e-02	9.40e-02
1	3.95e+00	1.60e-02	8.01e-02

Table 16: Runtime Metrics

havior, and non-locally determined non-linearity in the function  $m(x)$ . Unlike RDRs, the micro-bump reconfigurations are computationally more efficient but are limited to the plane as is illustrated by the run-times. However, Figure 7 illustrates that there is still room for numerical improvements to be made to the NEU-meta-algorithm which allows to take full advantage of Theorem 2.9 and that there may be more efficient way to incorporate Theorem 2.9 and Corollary 2.10 into other algorithms than is proposed in NEU.

Both the numerical implementations as well as the simulation studies show that the NEU algorithm makes simple algorithms competitive by embedding the universal approximation and universal reconfiguration properties into them. Future research could investigate the performance of the NEU meta-algorithm applied to other learning procedures such as clustering or classification tasks.

## 4 Conclusion

In this paper reconfigurations were introduced and shown to have the universal reconfiguration property introduced in Theorem 2.9, which stated that any dataset could be transformed into any other dataset using a reconfiguration. Applying the universal reconfiguration property to the graph of a continuous function, it was shown that reconfigurations also have the universal approximation property (Corollary 2.10) of neural networks.

The NEU meta-algorithm was introduced. NEU builds the universal reconfiguration and universal approximation properties into any objective learning algorithm. The resulting algorithm is found in three steps. First the optimal reconfiguration, which best relates a given dataset to the loss function defining the learning algorithm is learned. The old algorithm is then performed on the new reconfigured space and subsequently the prediction made by the learning algorithm is moved back to the original space by deconfiguration. Given any objective learning algorithm  $A$ , the algorithm NEU- $A$  was shown to outperform  $A$ , in the sense that it exhibits a lower validation-set loss.

The performance increase was justified both theoretically and supported empirically. The empirical experiments found that the variance of German bond yields was better explained with one NEU principal component than with 4 ordinary principal components. Likewise, the investigations of Apple stock price found that the residuals of the NEU-OLS algorithm was smaller than those of OLS, Ridge, LASSO, and ENET regression. The effectiveness of NEU-OLS as a non-parametric estimator was explored in three simulation studies which showed that using the universal reconfiguration and universal approximation properties of reconfigurations. It was confirmed that NEU-OLS is not only competitive with other non-parametric regression

methods but can better approximate functions with discontinuities, have non-locally determined behavior, or exhibit an oscillatory behavior.

A consequence of the construction of the NEU of an algorithm, is that once a correct geometry is learned for the algorithm given the data, the algorithm can be executed directly in the associated non-Euclidean space. This gave fast and simple algorithms such as linear regression higher validation set performance than their complicated and difficult to train Euclidean counterparts. These techniques can be applied outside of mathematical finance and we believe there are many applications in geonomics and mathematical imaging, where traditional machine learning algorithms are used.

The NEU meta-algorithm was shown to increase the explanatory and predictive power of an algorithm, both theoretically and through the implementations considered in this paper. However, NEU does reduce the speed of the original algorithm on the first run, when the reconfigurations are being learned. Future research needs to be done to find a way to minimize this computational shortcoming.

## References

- [1] 10 Major Companies Tied to the Apply Supply Chain (AAPL). <https://www.investopedia.com/articles/investing/090315/10-major-companies-tied-apple-supply-chain.asp>. Accessed: 2018-07-25.
- [2] O. Blanchard and J. Simon. The long and large decline in us output volatility. *Brookings papers on economic activity*, 2001(1):135–164, 2001.
- [3] L. Breiman. Bagging predictors. *Machine learning*, 24(2):123–140, 1996.
- [4] W. Cleveland and S. Devlin. Locally weighted regression: an approach to regression analysis by local fitting. *J. Am. Stat. Assoc.*, 83(403):596–610, 1988.
- [5] G. Cybenko. Approximation by superpositions of a sigmoidal function. *Math. Control Signals Syst.*, 2(4):303–314, 1989.
- [6] T. J. DiCiccio and B. Efron. Bootstrap confidence intervals. *Statist. Sci.*, 11(3):189–228, 1996. With comments and a rejoinder by the authors.
- [7] F. X. Diebold and C. Li. Forecasting the term structure of government bond yields. *J. Econometrics*, 130(2):337–364, 2006.
- [8] N. B. Erichson, P. Zeng, K. Manohar, S. L. Brunton, J. N. Kutz, and A. Y. Aravkin. Sparse principal component analysis via variable projection. *arXiv preprint arXiv:1804.00341*, 2018.
- [9] E. F. Fama and K. R. French. Industry costs of equity. *Journal of financial economics*, 43(2):153–193, 1997.
- [10] P. T. Fletcher. Geodesic regression and the theory of least squares on Riemannian manifolds. volume 105, pages 171–185, 2013.

- 
- [11] P. T. Fletcher, C. Lu, S. M. Pizer, and S. Joshi. Principal geodesic analysis for the study of nonlinear statistics of shape. *IEEE Trans. Med. Imaging*, 23(8):995–1005, 2004.
- [12] I. M. Gel’fand and G. E. Shilov. *Generalized functions. Vol. 2*. AMS Chelsea Publishing, Providence, RI, 2016.
- [13] C. Han and F. C. Park. A geometric GARCH framework for covariance dynamics. *SSRN Preprints*, 2016.
- [14] T. Hastie, R. Tibshirani, and J. Friedman. *The Elements of Statistical Learning*. Springer Series in Statistics. Springer, New York, second edition, 2009.
- [15] A. Hatcher. *Algebraic topology*. Cambridge University Press, Cambridge, 2002.
- [16] S. Hauberg, F. Lauze, and K. S. Pedersen. Unscented kalman filtering on riemannian manifolds. *J. Math. Imaging Vis.*, 46(1):103–120, 2013.
- [17] A. W. Knap. *Lie groups beyond an introduction*, volume 140. Springer, 2002.
- [18] J. M. Lee. *Introduction to Smooth Manifolds*, volume 218 of *Graduate Texts in Mathematics*. Springer, New York, second edition, 2013.
- [19] P. Liu. Approximation capabilities of multilayer feedforward regular fuzzy neural networks. *Appl. Math. J. Chinese Univ. Ser. B*, 16(1):45–57, 2001.
- [20] S. MacLane. *Categories for the working mathematician*. Springer-Verlag, New York-Berlin, 1971. Graduate Texts in Mathematics, Vol. 5.
- [21] J. A. Nelder and R. Mead. A simplex method for function minimization. *Comput. J.*, 7(4):308–313, 1965.
- [22] B. Pfaff. *Analysis of integrated and cointegrated time series with R*. Use R! Springer, New York, second edition, 2008.
- [23] F. Riesz. Elementarer beweis des egoroffschen satzes. *Monatshefte für Mathematik und Physik*, 35(1):243–248, 1928.
- [24] H. Royden and P. Fitzpatrick. *Real analysis*. Printice-Hall Inc, New Jersey, fourth edition, 2010.
- [25] W. Rudin. *Principles of mathematical analysis*. International series in pure and applied mathematics. McGraw-Hill, 3 edition, 1976.
- [26] R. E. Schapire. The strength of weak learnability. *Mach. Learn.*, 5(2):197–227, 1990.
- [27] B. Schölkopf, A. Smola, and K.-R. Müller. Nonlinear component analysis as a kernel eigenvalue problem. *Neural computation*, 10(5):1299–1319, 1998.
- [28] E. H. Spanier. *Algebraic topology*. Springer-Verlag, New York, 1995.
- [29] K. Stoller. The world’s largest tech companies 2018: Apple, samsung take top spots again. *Frobes*, Jun 2018.

- [30] N. R. Swanson. Money and output viewed through a rolling window. *Journal of monetary Economics*, 41(3):455–474, 1998.
- [31] R. Tibshirani. Regression shrinkage and selection via the lasso. *J. R. Stat. Soc. Series B. Stat. Methodol*, pages 267–288, 1996.
- [32] A. N. Tikhonov. Solution of incorrectly formulated problems and the regularization method. *Dokl. Akad. Nauk. SSSR*, 151:501–504, 1963.
- [33] H. Xu, C. Caramanis, and S. Mannor. Robust regression and LASSO. *IEEE Trans. Inform. Theory*, 56(7):3561–3574, 2010.
- [34] H. Zou and T. Hastie. Regularization and variable selection via the elastic net. *Journal of the Royal Statistical Society: Series B (Statistical Methodology)*, 67(2):301–320, 2005.
- [35] H. Zou and T. Hastie. Regularization and variable selection via the elastic net. *J. R. Stat. Soc. Series B. Stat. Methodol*, 67(2):301–320, 2005.
- [36] H. Zou, T. Hastie, and R. Tibshirani. Sparse principal component analysis. *J. Comput. Graph. Statist.*, 15(2):265–286, 2006.

## A Regularity Conditions

This appendix contains a list of all the technical regularity conditions used in this paper.

**Regularity Condition A.1** (Regularity Condition) *For every choice of hyper-parameters  $\gamma \in \Gamma$  and every data-sample  $X \in \mathbb{R}^{DN_I}$  the map*

$$\begin{aligned} \mathcal{L}_I^{N_I}(\cdot, \phi(\cdot|X^I); \gamma | X^I) : \mathbb{R}^d &\rightarrow \mathbb{R} \\ \beta &\mapsto \mathcal{L}_I^{N_I}(\beta, \phi(\beta|X^I); \gamma | X^I), \end{aligned}$$

*has a, possibly not unique, infimum.*

**Regularity Condition A.2** *Let  $(X^I, X^O)$  be a pair of training and validation datasets.*

- (i) *For every hyper-parameter  $\gamma \in \Gamma$ , there exists a unique optimal parameter  $\beta(\gamma)$  in  $\mathbb{R}^d$  such that for all other parameters  $\tilde{\beta}$  in  $\mathbb{R}^d$*

$$\mathcal{L}_I^{N_I}(\beta(\gamma), \phi(\beta(\gamma)|X^I); \gamma | X^I) < \mathcal{L}_I^{N_I}(\tilde{\beta}, \phi(\tilde{\beta}|X^I); \gamma | X^I),$$

- (ii) *There exists a unique hyper-parameter  $\hat{\gamma}$  in  $\Gamma$  such that for every other hyper-parameter  $\gamma$  in  $\Gamma$*

$$\mathcal{L}_O^{N_O}(\beta(\hat{\gamma}), \phi(\beta(\hat{\gamma})|X^O); \hat{\gamma} | X^O) < \mathcal{L}_O^{N_O}(\beta(\gamma), \phi(\beta(\gamma)|X^O); \gamma | X^O).$$

**Regularity Condition A.3** *The pair  $\left(\left\{\Phi(X_j^I)\right\}_{j=1}^{N_I}, \left\{\Phi(X_i^O)\right\}_{i=1}^{N_O}\right)$  is in  $\text{Dom}(\mathcal{L}_I, \mathcal{L}_O, \Gamma, \phi)$ .*

**Regularity Condition A.4**  $D > 1$  and there exists  $(\tilde{X}_I, \tilde{X}_O) \in \text{Dom}(\mathcal{L}_I, \mathcal{L}_O, \Gamma, \phi)$  such that  $\mathcal{P}(\mathcal{L}_I, \mathcal{L}_O)(\tilde{X}_I, \tilde{X}_O) < \mathcal{P}(\mathcal{L}_I, \mathcal{L}_O)(X^I, X^O)$ .

**Regularity Condition A.5** There exists a regular convex compact set  $V$  containing the compact set  $[K \times f(K)] \cup [K \times g(K)]$  such that for every  $\theta \in \Theta$ , the reconfiguration map  $\xi(\cdot|\theta)$  on  $\text{int}(V)$  of dimension  $D_2$ . For every  $\theta \in \Theta$ ,  $\xi(\cdot|\theta)$  the partial derivatives of  $\xi$  are uniformly bounded by 1.

## B Technical Proofs

*Proof of Proposition 2.3.* Since additive conjugation by  $c$  is its own inverse, we may assume that  $c = 0$ . For any  $X \in \mathfrak{so}(D)$ ,  $\exp(X)$  is a rotation matrix and is therefore an isometry from  $\mathbb{R}^D$  onto itself. Therefore,

$$\|\exp(f(\|x\|)X)x\| = \|x\|, \quad (\text{B.1})$$

from which it follows that

$$f(\|x\|) = f(\|\exp(f(\|x\|)X)x\|). \quad (\text{B.2})$$

Moreover, since  $\exp$  is a group homomorphism

$$\exp(X + Y) = \exp(X)\exp(Y). \quad (\text{B.3})$$

Combining Equations (B.2) and (B.3) we obtain

$$\begin{aligned} I &= (\exp(f(\|x\|)X)x - f(\|x\|)X)x \\ &= (\exp(f(\|x\|)X)x) (\exp(f(\|x\|)X)(-X))x \\ &= (\exp(f(\|x\|)X)x) (\exp([f(\|x\|)X])(-X))x. \end{aligned} \quad (\text{B.4})$$

Therefore Definition 2.1 (i) holds.

The maps  $\exp$  and  $\phi$  are infinitely differentiable, see [17] and [12] respectively. Moreover, since  $\|\cdot\|$  and  $\pm c$ , therefore  $\Psi(\cdot|\theta)$  and  $\Phi(\cdot|\theta)$  are infinitely differentiable. Therefore Definition 2.1 (ii) and (iii) hold.

Let  $c$  be the midpoint between  $x$  and  $y$ , moreover let  $\epsilon \triangleq \|x - y\|$  and  $\sigma \triangleq \frac{\|x - z\| + \epsilon}{2}$ . Therefore, for any choice of  $X$  in  $\mathfrak{so}(D)$ ,  $\xi(z|(c, \sigma, X)) = z$ . Since  $\exp$  maps  $\mathfrak{so}(D)$  onto the set  $SO(D)$  which is the collection of all maps from the  $D$ -sphere onto itself and  $x, y$  lie on the same sphere centered at  $c$  of radius  $\epsilon$ , then there exists  $X$  in  $\mathfrak{so}(D)$  for such that  $\xi(x|(c, \sigma, X))$  is a rotation taking  $x$  to  $y$ . Therefore Definition 2.1 (iv) holds.

For a triple  $(c, \sigma, 0)$ , the application of the map  $\xi(x|(c, \sigma, X))$  becomes multiplication by the identity matrix in this case, hence (v) holds.  $\square$

*Proof of Proposition 2.6.* Definition 2.1 (i,ii,iii,v) hold analogously to the proof of Proposition 2.3. To see Definition 2.1 (iv) note that if  $c$  is the midpoint between  $x$  and  $y$  and  $\sigma$  is taken to be  $d(x, y)$  then  $\xi$  is the identity function outside the ball centered at  $c$  of radius  $\sigma$ , therefore  $\xi(z|(c, \sigma, X)) = z$  for any  $X \in \mathbb{R}$ . Taking  $X = (x - y)/\psi(\|x - y\|; \sigma)$  establishes Definition 2.1 (iv).  $\square$

The proof of Theorem 2.9 relies on the construction of a particular curve described by the next Lemma.

**Lemma B.1.** Let  $D > 1$  and let  $x_1, \dots, x_n, x, z$  be distinct points in  $\mathbb{R}^D$  and let  $\Delta \in (0, \infty]$ . Then there exists positive integers  $n, K$  and a curve  $\gamma$  from  $x$  to  $z$  satisfying

- (i)  $\gamma$  is rectifiable with length  $l$ ,
- (ii)  $\gamma(0) = x$  and  $\gamma(1) = z$ ,
- (iii)  $0 < \frac{1}{n} < \min_{\substack{t \in [0,1] \\ i,j=1,\dots,N}} \{\|\gamma(t) - x_i\|, \Delta\}$ ,
- (iv)  $\gamma([0, 1]) = \gamma([0, 1]) \cap \left[ \bigcup_{k=1}^K \text{Ball} \left( \gamma \left( \frac{k}{K} \right); \frac{1}{K} \right) \right]$ ,
- (v)  $\emptyset = \bigcup_{i=2}^n \{x_i\} \cap \left[ \bigcup_{k=1}^K \text{Ball} \left( \gamma \left( \frac{k}{K} \right); \frac{1}{K} \right) \right]$ .

*Proof of Lemma B.1.* The existence of such a curve is equivalent to looking for a smooth curve inside the open set  $\mathbb{R}^D - \bigcup_{i=1}^N \{X_i\} \cup \left[ \bigcup_{i=1}^N \{\tilde{X}_i\} \right]$ , which is in-turn equivalent to the open subset  $\mathbb{R}^D - \bigcup_{i=1}^N \{X_i\} \cup \left[ \bigcup_{i=1}^N \{\tilde{X}_i\} \right]$  of  $\mathbb{R}^D$  being simply connected. More generally, let  $X_N$  be  $\mathbb{R}^D$  with the  $N$ -distinct points  $\{x_1, \dots, x_N\}$  deleted.

Simply connectedness of  $X_N$  will be proven by strong induction on  $N$ . If  $N = 1$  then  $X_N$  is simply connected since  $X_1$  is homeomorphic to  $\mathbb{R}^D - \{0\}$  which is a deformation retract of the  $(D-1)$ -sphere  $S^{D-1}$  (see [15, Excerise 0.2]). Since homeomorphisms and deformation retractions induce chain homotopies in their associated chain complexes (see [15, Chapter 2.1]) and since the homology functors  $H_n$  are invariant under chain homotopies (see [15, Proposition 2.1.2]), then there are group isomorphism

$$H_n(X_1) \cong H_n(\mathbb{R}^D - \{0\}) \cong H_n(S^{D-1}) \cong \begin{cases} \mathbb{Z} & \text{if } n = D, 0 \\ 0 & \text{else.} \end{cases}$$

where the last isomorphism is computed in [28, Theorem 4.6.6]<sup>4</sup>. Applying [28, Lemma 4.4.7] implies that  $X_1$  is path-connected. Suppose that  $X_N$  is path connected for some  $N \geq 1$ . Since the interiors of the sets<sup>5</sup>  $A \triangleq \mathbb{R}^D - \bigcup_{i=2}^N \{x_i\}$ ,  $B \triangleq \mathbb{R}^D - \{x_1\}$  cover  $\mathbb{R}^D$  and their intersection is  $X_N$ . The Mayer-Vietoris sequence (see [28, page 190]) implies that there is a long-exact sequence in singular homology

$$0 \cong H_0(\mathbb{R}^D) \leftarrow H_0(\mathbb{R}^D) \leftarrow H_0(A) \oplus H_0(B) \leftarrow H_0(A \cap B) \leftarrow H_1(\mathbb{R}^D). \quad (\text{B.5})$$

By [28, Lemma 4.4.1],  $\mathbb{R}^D$  is contractible, therefore  $H_0(\mathbb{R}^D) \cong \mathbb{Z}$  and  $H_n(\mathbb{R}^D) \cong 0$  if  $n > 0$ . Applying the strong induction hypothesis that  $H_0(A) \cong \mathbb{R} \cong H_0(B)$ , it follows that

$$0 \cong \mathbb{Z} \leftarrow \mathbb{Z} \oplus \mathbb{Z} \leftarrow H_0(A \cap B) \leftarrow 0$$

<sup>4</sup>Actually, it is computed for the reduced homology. However, [28, Lemma 4.3.1] permits the translation into singular homology.

<sup>5</sup>The interior of an open set is itself.



is an exact sequence of groups. The Splitting Lemma implies that

$$\mathbb{Z} \cong \mathbb{Z} \oplus H_0(A \cap B);$$

therefore  $H_0(A \cap B) = \mathbb{Z}$ , hence  $A \cap B$  is path connected by [28, Lemma 4.4.7]. Since  $A \cap B = X_d$ , it follows that  $X_d$  is path connected. Picking  $x_1, \dots, x_N$  to be the data-points  $\bigcup_{i=1}^N \{X_i\} \cup \bigcup_{i=1}^N \{\tilde{X}_i\}$  it follows that there exists a path  $\tilde{\gamma}$  which is interior to  $\mathbb{R}^D - \bigcup_{i=1}^N \{X_i\} \cup \bigcup_{i=1}^N \{\tilde{X}_i\}$  connecting  $X_1$  to  $\tilde{X}_1$ . This completes the induction step.

Since  $\tilde{\gamma}([0, 1])$  is compact there exists a finite open cover  $\{V_j\}_{j=1}^J$  of  $\tilde{\gamma}([0, 1])$ . Therefore, the open sets  $\left\{W_j \triangleq V_j \cap \left[\mathbb{R}^D - \bigcup_{i=1}^N \{X_i\} \cup \bigcup_{i=1}^N \{\tilde{X}_i\}\right]\right\}_{j=1}^J$  is a finite collection of sets diffeomorphic to  $\mathbb{R}^D$ , via some diffeomorphism  $\{\phi_j\}_{j=1}^J$ . Therefore each  $\phi_j \circ \gamma|_{W_j}$  defines a continuous path from into  $\mathbb{R}^D$ . The Whitney Approximation Theorem (see [18, Theorem 6.12]) implies that for each  $j$  in  $\{1, \dots, J\}$  there exists a smooth curve  $\tilde{\gamma}_j$  which is  $\delta$ -close to  $\phi_j \circ \gamma$ ; where

$$\delta \triangleq \min_{i=2, \dots, N} \frac{\left\{ \|X_i - \tilde{\gamma}(t)\|, \|\tilde{X}_i - \tilde{\gamma}(t)\| \right\}}{2}.$$

Therefore the composition  $\phi_j^{-1} \circ \tilde{\gamma}_j$  a piecewise-smooth curve, denoted by  $\gamma$ , which joins  $X_1$  to  $\tilde{X}_1$  and is contained entirely within  $\mathbb{R}^D - \left[\bigcup_{i=1}^N \{X_i\} \cup \bigcup_{i=1}^N \{\tilde{X}_i\}\right]$ . Since every piecewise-smooth curve is rectifiable, by definition of arc-length  $\gamma$  has finite arc-length, which we denote by  $l$ . This establishes (i) and (ii).

Define  $\epsilon > 0$  as

$$\epsilon \triangleq \min_{i=2, \dots, N} \frac{\left\{ \|X_i - \gamma(t)\|, \|\tilde{X}_i - \gamma(t)\| \right\}}{2}.$$

By the Archimedean property of  $\mathbb{R}$ , there exists a positive integer  $n$  for which  $0 < \frac{1}{n} < \min\{\epsilon, l\}$ . Observe that the definitions of  $\epsilon$  and  $\gamma$  imply that

$$\begin{aligned} \gamma([0, 1]) &= U \cap \gamma([0, 1]), \\ \emptyset &= \bigcup_{i=2}^N \{X_i, \tilde{X}_i\} \cap U, \\ U &\triangleq \bigcup_{k=1}^n \text{Ball} \left( \gamma \left( \frac{k}{n} \right); \frac{1}{n} \right); \end{aligned}$$

therefore (iii) – (v) hold.  $\square$

*Proof of Theorem 2.9.*  $\mathcal{M}$  is diffeomorphic to  $\mathbb{R}^D$  it may be assumed without loss of generality that  $\mathcal{M} = \mathbb{R}^D$ . Similarly, since open star-shaped domains in  $\mathbb{R}^D$  of dimension  $D$  are diffeomorphic to  $\mathbb{R}^D$  then without loss of generality it may also be assumed that  $\mathcal{S} = \mathbb{R}^D$ . The case that  $X = \tilde{X}$  must hold with  $K = 1$  by choosing  $\theta_1$  to be any element of  $\Theta_0$ , which is possible since  $\Theta_0$  is non-empty. Assume without loss of generality that the collections  $X$  and  $\tilde{X}$  are formed of distinct elements.

We proceed by induction. Suppose that  $N = 1$ . Let  $\epsilon \triangleq 2\|X_1 - \tilde{X}_1\|$  and let  $Z$  be any point in  $\mathbb{R}^D$  for which  $\|Z - X_1\| > \epsilon$ . Then the local-transience property of  $\xi$  implies that there exists  $\theta_1 \in \Theta$  such that

$$\xi(X_1|\theta_1) = \tilde{X}_1; \xi(Z|\theta) = Z.$$

Suppose now that the claim holds for  $N \geq 1$ . In the notation of Lemma B.1, let  $x_1, \dots, x_n = X_2, \dots, X_N, \tilde{X}_2, \dots, \tilde{X}_N$ ,  $x = X_1$ , and  $z = \tilde{X}_1$ . Since there exists a rectifiable curve  $\gamma$  connecting  $x$  to  $z$  and  $\gamma$  is uniformly bounded away from each  $x_i$  by a distance of at least  $\frac{1}{n}$ , where  $\frac{1}{n}$  is set to be less than the locality  $\Delta$ , then there exists a set of open balls  $\{Ball(\gamma(\frac{k}{K}); \frac{1}{K})\}_{k=1}^K$  covering  $\gamma$  which are separated from the points  $x_1, \dots, x_n$ , by a distance of at least  $\frac{1}{n}$ . The local transience property of  $\xi$  implies that there exist  $\theta_1^1, \dots, \theta_K^1$  in  $\Theta$  satisfying

$$\begin{aligned} \xi\left(\gamma\left(\frac{k-1}{K}\right) \middle| \theta_k^1\right) &= \gamma\left(\frac{k}{K}\right) \\ \xi(x_i|\theta_k^1) &= x_i, \end{aligned}$$

for every  $i$  in  $\{1, \dots, n\}$  and every  $k$  in  $\{1, \dots, K\}$ .

Repeating this construction and process for every data-point  $X_i$  we find a list of parameters

$$\theta_1^1, \dots, \theta_{K_1}^1, \theta_1^2, \dots, \theta_{K_2}^2, \dots, \theta_{K_N}^N,$$

such that

$$\mathbb{X}(X_j|\theta_1^i, \dots, \theta_{K_i}^i) = \begin{cases} \tilde{X}_i & \text{if } i = j \\ X_j & \text{else.} \end{cases}$$

Definition 2.1[(iv)] implies that any  $Z$  not in  $\cup_{k=1}^K Ball(\gamma(\frac{k}{K}); \frac{1}{n})$  must remain fixed by  $\mathbb{X}$ .  $\square$

*Proof of Corollary 2.10.* Let  $\mathcal{S}$  be an open subset of  $\mathbb{R}^{D_1}$ , diffeomorphic to  $\mathbb{R}^{D_1}$  and let  $Q$  be a countable subset of  $\mathcal{S}$ . Let  $\{x_i\}_{i \in \mathbb{N}}$  be an enumeration of  $Q$  and define the sequences of points  $\{X_i\}_{i \in \mathbb{N}}$  and  $\{\tilde{X}_i\}_{i \in \mathbb{N}}$  in  $\mathbb{R}^{D_1+D_2}$  by

$$\begin{aligned} X_i &\triangleq (x_i, g(x_i)) \\ \tilde{X}_i &\triangleq (x_i, f(x_i)). \end{aligned}$$

Since  $\mathbb{R}^{D_1+D_2}$  is of dimension at least 2 and  $\mathcal{S}$  is diffeomorphic to  $\mathbb{R}^{D_1}$ , then for every  $n \in \mathbb{N}$  Theorem 2.9 applies to the sets of points  $\{X_i\}_{i=1}^n$  and  $\{\tilde{X}_i\}_{i=1}^n$  in  $\mathbb{R}^{D_1+D_2}$ . Therefore for every  $n \in \mathbb{N}$  there exists  $\theta_1^n, \dots, \theta_{N_n}^n \in \Theta$  such that

$$\mathbb{X}(X_i|\theta_1^n, \dots, \theta_{N_n}^n) = \tilde{X}_i; i = 1, \dots, n. \quad (\text{B.6})$$

Define the sequence of functions  $\{f_n\}_{n \in \mathbb{N}}$  from  $\mathcal{S}$  to  $\mathbb{R}^{D_2}$  by

$$f_n(x) \triangleq p \circ \mathbb{X}((x, g(x))|\theta_1^n, \dots, \theta_{N_n}^n), \quad (\text{B.7})$$

where  $p$  is the second canonical projection on  $\mathbb{R}^{D_1} \times \mathbb{R}^{D_2}$  onto  $\mathbb{R}^{D_2}$ . From equation (B.6), it follows that the sequence  $\{f_n\}_{n \in \mathbb{N}}$  converge point-wise to  $f$  on  $Q$ . This establishes the  $\epsilon = 0$  case.

Now assume that  $\epsilon > 0$ . Since  $\mathbb{P}$  is a probability measure,  $Q$  is of finite  $\mathbb{P}$ -measure. Therefore  $\{f_n\}_{n \in \mathbb{N}}$  is a sequence of Borel-measurable functions over a set of finite  $\mathbb{P}$ -measure converging point-wise to the Borel-measurable function  $f$ , where  $f$  takes values in the separable metric space  $(\mathbb{R}^{D_2}, d_E)$ . Here  $d_E$  is the Euclidean metric on  $\mathbb{R}^{D_2}$ . Hence, Egorov's Theorem (see [23] for details) gives the existence of the set  $\mathcal{S}_\epsilon$  as well as the uniform convergence of the sequence  $\{f_n\}_{n \in \mathbb{N}}$  to  $f$  on  $\mathcal{S}_\epsilon$ . This establishes the case where  $\epsilon > 0$ .  $\square$

*Proof of Corollary 2.11.* Let  $\mathcal{F}$  be the collection of functions from  $K$  to  $\mathbb{R}^{D_2}$  whose members are of the form

$$p \circ \mathbb{X}((x, g(x)) | \theta_1, \dots, \theta_N),$$

where  $\theta_1, \dots, \theta_N \in \Theta$  and  $p$  is the second canonical projection of  $\mathbb{R}^{D_1+D_2}$  onto  $\mathbb{R}^{D_2}$ . The Arzela-Ascoli, will be used to conclude that every sequence in  $\mathcal{F}$  has a convergent subsequence in  $\mathcal{F}$ . The equicontinuity of  $\mathcal{F}$  will be established using [25, Theorem 9.19], by first showing that every map in  $\mathcal{F}$  is continuously differentiable with first partial derivatives uniformly bounded by 1, and subsequently that every function in  $\mathcal{F}$  is uniformly bounded by 1.

Since  $g$  is continuously differentiable, the projection map is smooth, and  $\xi$  is continuously differentiable, it follows that any function in  $\mathcal{F}$  is continuously differentiable. The uniform bound on the partial derivatives of the functions in  $\mathcal{F}$  is established using induction. The base case is established by the assumption that the partial derivatives of  $\xi(x|\theta)$  are uniformly bounded by 1 for every  $\theta \in \Theta$ . Without loss of generality the inductive step will be shown for the partial derivative with respect to the first coordinate  $x_1$ , by induction on  $N$

$$\begin{aligned} \left\| \frac{\partial \mathbb{X}(x|\theta_1, \dots, \theta_N)}{\partial x_1} \right\| &= \left\| \frac{\partial \mathbb{X}(x|\theta_1, \dots, \theta_{N-1})}{\partial x_1} \frac{\partial \xi(\mathbb{X}(x|\theta_1, \dots, \theta_{N-1}) | \theta_N)}{\partial x_1} \right\| \\ &\leq \left\| \frac{\partial \xi(x|\theta_N)}{\partial x_1} \right\| \left\| \frac{\partial \xi(\mathbb{X}(x|\theta_1, \dots, \theta_{N-1}) | \theta_N)}{\partial x_1} \right\| \\ &\leq 1. \end{aligned}$$

Therefore for every  $\theta_1, \dots, \theta_N$ , the reconfiguration  $\mathbb{X}(x|\theta_1, \dots, \theta_N)$  has first derivative uniformly bounded by 1. Since the canonical projection  $p$  is smooth and its derivative is bounded by 1, it follows that any  $f \in \mathcal{F}$  is continuously differentiable with first partial derivatives uniformly bounded by 1.

Since  $\xi$  satisfies regularity condition A.5, the diameter  $\text{diam}(V)$  is finite since  $V$  is compact. This implies that  $\xi$  is bounded. The uniform bound on the functions in  $\mathcal{F}$  follows from the following computation

$$\begin{aligned} \|p \circ \mathbb{X}(x|\theta_1, \dots, \theta_N)\| &\leq \|\mathbb{X}(x|\theta_1, \dots, \theta_N)\| \\ &= \|\xi(\mathbb{X}(x|\theta_1, \dots, \theta_{N-1}) | \theta_N)\| \\ &\leq \text{diam}(V) < \infty. \end{aligned}$$

Since  $K$  is convex,  $\mathcal{F}$  is an equicontinuous family of functions on  $K$ .

Therefore, the hypothesis for the Arzela-Ascoli theorem hold and  $\mathcal{F}$  is relatively compact in  $C^1(\mathbb{R}^{D_1}; \mathbb{R}^{D_2})$ . In particular, this implies that a subsequence of the sequence functions  $\{f_n\}_{n \in \mathbb{N}}$

of Equation (B.7) uniformly converge to a continuously differentiable function  $\tilde{f}$  on  $K$ , moreover on  $\text{int}(K)$ .

Since  $K$  is convex, the interior of any convex set is itself convex, any convex set is a star-shaped domain, and every star-shaped domain is diffeomorphic to the Euclidean space of the same dimension, then  $\text{int}(K)$  is diffeomorphic to the Euclidean space of the same dimension. Since  $K$  is regular closed set, then  $\dim(\text{int}(K)) = \dim(K) = D_1$ , therefore  $\text{int}(K)$  is diffeomorphic to  $\mathbb{R}^{D_1}$ . Hence, Corollary 2.10 can be applied to conclude that on the countable subset  $Q$  of  $\text{int}(K)$ ,

$$\tilde{f}(x) = f(x). \tag{B.8}$$

Since  $\mathbb{R}^{D_1}$  with its Euclidean topology, is separable then [24, Proposition 26] implies that  $\text{int}(K)$  is also separable. Therefore,  $Q$  may be taken to be a countable dense subset of  $\text{int}(K)$ . Since  $K$  is regular, then

$$\text{cl}(Q) = \text{cl}(\text{int}(K)) = K,$$

hence  $Q$  is dense in  $K$ . Since  $K$  is compact and both  $\tilde{f}, f$  are continuous on  $K$  then they are uniformly continuous. Since uniformly continuous functions are uniquely determined by their value on dense subsets, Equation (B.8) implies that  $\tilde{f} = f$  on  $K$ .  $\square$